© 2022. Published by The Company of Biologists Ltd | Development (2022) 149, dev200021. doi:10.1242/dev.200021

RESEARCH ARTICLE

FGFR2 signaling enhances the SHH-BMP4 signaling axis in early ureter development

Max Meuser[1,*], Lena Deuper[1,*], Carsten Rudat[1], Nurullah Aydoğdu[1], Hauke Thiesler[2], Patricia Zarnovican[2], Herbert Hildebrandt[2], Mark-Oliver Trowe[1] and Andreas Kispert[1,‡]

ABSTRACT

The patterned array of basal, intermediate and superficial cells in the urothelium of the mature ureter arises from uncommitted epithelial progenitors of the distal ureteric bud. Urothelial development requires signaling input from surrounding mesenchymal cells, which, in turn, depend on cues from the epithelial primordium to form a layered fibro-muscular wall. Here, we have identified FGFR2 as a crucial component in this reciprocal signaling crosstalk in the murine ureter. Loss of *Fgfr2* in the ureteric epithelium led to reduced proliferation, stratification, intermediate and basal cell differentiation in this tissue, and affected cell survival and smooth muscle cell differentiation in the surrounding mesenchyme. Loss of *Fgfr2* impacted negatively on epithelial expression of *Shh* and its mesenchymal effector gene *Bmp4*. Activation of SHH or BMP4 signaling largely rescued the cellular defects of mutant ureters in explant cultures. Conversely, inhibition of SHH or BMP signaling in wild-type ureters recapitulated the mutant phenotype in a dose-dependent manner. Our study suggests that FGF signals from the mesenchyme enhance, via epithelial FGFR2, the SHH-BMP4 signaling axis to drive urothelial and mesenchymal development in the early ureter.

KEY WORDS: FGF, FGFR2, Urothelium, Ureter, Epithelial differentiation, SHH, BMP4

INTRODUCTION

The urothelium is a stratified epithelium that lines the inner surface of the urinary drainage system. In the ureter and bladder, it consists of three major cell types that are organized in radial layers of variable thickness. Large binucleated superficial (S-) or umbrella cells border the lumen and primarily account for the essential barrier function of the tissue. They are sealed by tight junctions and are covered by crystalline plaques of specialized surface proteins: uroplakins (UPKs). Underneath, much smaller intermediate (I) cells form one to several layers depending on species and organ, and serve as precursors for S and basal (B) cells. These small B cells abundantly express keratin 5 (KRT5) and provide an anchor to the basal lamina and the surrounding fibro-muscular wall (Dalghi et al., 2020; Wang et al., 2017).

This urothelial cytoarchitecture derives from highly coordinated proliferation, patterning and differentiation processes that act on epithelial progenitors (the cloacal epithelium in the bladder, the distal ureteric bud in the ureter) starting around embryonic day (E) 10.5 of mouse development (Wang et al., 2017; Yamany et al., 2014). After an initial phase of proliferative expansion, the mono-layered epithelial primordia stratify concomitant with the expression of the transcription factor ΔNP63, indicating I-cell differentiation. After 2 days, the adluminal layer starts to express S-cell markers. B-cell differentiation occurs 2 additional days later (Bohnenpoll et al., 2017a; Gandhi et al., 2013).

Urothelial development in the bladder and ureter does not occur in a cell-autonomous fashion but requires signaling input from adjacent mesenchymal cells, which, in turn, depend on signals from the epithelial primordium to develop into a layered fibro-muscular wall (Balsara and Li, 2017; Bohnenpoll and Kispert, 2014; Cunha et al., 1991; Wang et al., 2017). To date, members of three classes of secreted proteins have been characterized as essential mesenchymal signals for urothelial development: bone morphogenetic protein 4 (BMP4), retinoic acid (RA) and fibroblast growth factors (FGFs). Analysis of conditionally mutant mice showed that *Bmp4* is required in the ureteric mesenchyme (UM) for stratification and cytodifferentiation of the adjacent ureteric epithelium (UE) (Mamo et al., 2017). Expression of *Bmp4* in the UM depends on the transcription factor FOXF1, which, in turn, requires input from an epithelial sonic hedgehog (SHH) signal. SHH acts through this FOXF1-BMP4 axis to control not only epithelial differentiation but also survival, proliferation and smooth muscle cell (SMC) differentiation of surrounding mesenchymal cells, thereby coupling the development of the two tissues (Bohnenpoll et al., 2017c; Yu et al., 2002). *Bmp4* expression receives an additional input from the canonical (CTNNB1-dependent) branch of WNT signaling triggered by WNT ligands from the UE (Trowe et al., 2012). RA has been found to prevent the differentiation of B and S cells in ureter explant cultures (Bohnenpoll et al., 2017b). In the bladder, loss of RA signaling led to a single-layered epithelium with B cells, indicating that, in this context, RA signaling is required for S-cell specification (Gandhi et al., 2013).

Embryos deficient for *Fgf7* exhibit a thinning of the bladder urothelium, particularly of the I-cell layers. *In vitro*, FGF7 stimulated I-cell proliferation and delayed their differentiation into S cells (Tash et al., 2001). Furthermore, FGF10 was shown to act as a mitogen for urothelial cells (Bagai et al., 2002; Zhang et al., 2006). How these mesenchymal FGF signals are transmitted to the epithelium and what targets their signaling pathway has is unknown, as is the interaction of FGF signaling with other signaling systems in this context.

Here, we set out to analyze the role of FGF signaling in urothelial development using the murine ureter as a model. We provide genetic evidence that FGFR2 signaling enhances SHH-BMP4 signaling activity, which is essential for epithelial and mesenchymal proliferation, and differentiation in this organ.

[1]Institute of Molecular Biology, Medizinische Hochschule Hannover, 30625 Hannover, Germany. [2]Institute of Clinical Biochemistry, Medizinische Hochschule Hannover, 30625 Hannover, Germany.
*These authors contributed equally to this work

‡Author for correspondence (kispert.andreas@mh-hannover.de)

A.K., 0000-0002-8154-0257

Handling Editor: Liz Robertson
Received 16 July 2021; Accepted 9 December 2021

Development (2022) 149, dev200021. doi:10.1242/dev.200021

RESULTS

Fgfr2 is transiently expressed in the epithelium of the developing ureter

Previous work described expression of *Fgf7* and *Fgf10* in the early bladder mesenchyme, while expression of *Fgfr1* and *Fgfr2* was found in the adjacent cloacal epithelium (Cancilla et al., 1999; Dudley et al., 1999; Peters et al., 1992; Tash et al., 2001). To determine whether the expression of these FGF signaling components is conserved in ureter development, we performed *in situ* hybridization analysis on transverse sections of the trunk region of E12.5 to E18.5 wild-type embryos (Fig. 1). At E12.5, both *Fgfr1* and *Fgfr2* were expressed in the UE and UM, *Fgfr2* more strongly and enhanced in the UE. Expression of both genes continued at lower levels at E14.5 and disappeared in both tissues until E18.5. Expression of *Fgf7* and *Fgf10*, the encoded proteins of which predominantly bind to the epithelial (IIIb) isoform of FGFR2 (Igarashi et al., 1998; Jans, 1994; Ornitz and Itoh, 2015), occurred weakly in the UM, particularly at E14.5 (Fig. 1A). We did not detect specific expression of other FGF ligand genes in the UM or the UE from E12.5 to E16.5 (Fig. S1). Importantly, *Spry1* and *Spry2*, target genes of the FGF signaling pathway (Hanafusa et al., 2002), were strongly expressed in the UE at E12.5 and at E14.5 (Fig. 1B). These findings suggest that mesenchymal FGF7 and FGF10 predominantly activate epithelial FGFR2 signaling in early ureter development.

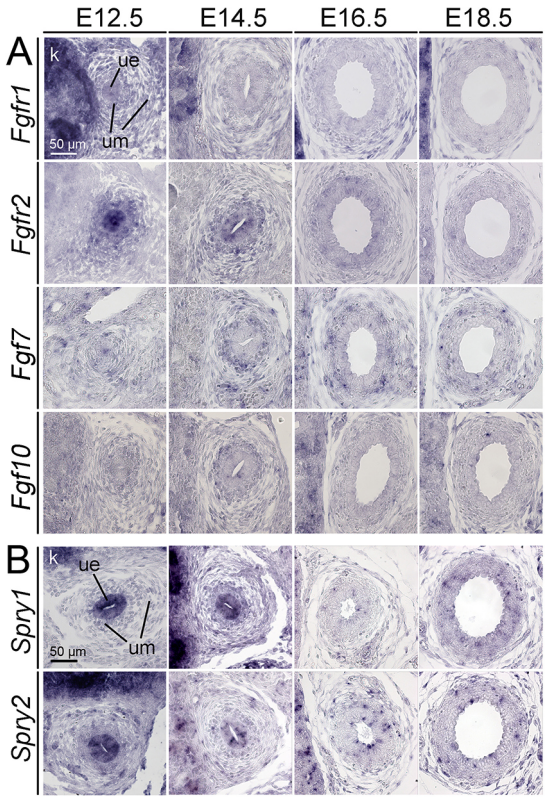

Fig. 1. FGF signaling during embryonic ureter development. (A,B) RNA *in situ* hybridization analysis on transverse sections through the posterior trunk region at the proximal (kidney) level of the ureter of wild-type embryos from E12.5 to E18.5 for expression of two FGFR genes (*Fgfr1* and *Fgfr2*) and two genes encoding FGF ligands (*Fgf7* and *Fgf10*) (A), and of two transcriptional targets of FGF signaling (*Spry1* and *Spry2*) (B). $n \geq 3$ for all probes, stages and genotypes. k, kidney; ue, ureteric epithelium; um, ureteric mesenchyme.

Loss of *Fgfr2* in the UE leads to hydroureter formation and absence of I- and B-cell layers in the urothelium at birth

To explore the specific role of *Fgfr1* and/or *Fgfr2* in the UE, we used a conditional gene inactivation approach with floxed alleles of *Fgfr1* and *Fgfr2* (Hoch and Soriano, 2006; Yu et al., 2003), and a *Pax2-cre* line that mediates recombination in the nephric duct, the precursor of the UE and of the renal collecting duct system (Bohnenpoll et al., 2017a; Trowe et al., 2011). We mated *Pax2-cre/+;Fgfr1*$^{fl/+}$*;Fgfr2*$^{fl/+}$ males with *Fgfr1*$^{fl/fl}$*;Fgfr2*$^{fl/fl}$ females and analyzed the genotype distribution at different time points of embryogenesis. At all stages, *Pax2-cre/+;Fgfr1*$^{fl/fl}$*;Fgfr2*$^{fl/+}$ embryos were found at approximately one-half of the expected frequency, and *Pax2-cre/+;Fgfr1*$^{fl/fl}$*;Fgfr2*$^{fl/fl}$ embryos at a quarter, indicating that homozygous loss of *Fgfr1* accounts for lethality before E12.5, which is further enhanced by removal of *Fgfr2* function (Table S1). Notably, expression of *Spry1* and *Spry2* was strongly reduced at E12.5 and E14.5 in the UE of embryos with loss of two alleles of *Fgfr2*, indicating that FGFR1 does not contribute in a major fashion to FGF signaling in this tissue (Fig. S2).

Morphological inspection of whole urogenital systems at the end of embryonic development, at E18.5, revealed that conditional loss of two and more alleles of *Fgfr1* and *Fgfr2* led with variable severity and penetrance to sex-independent hydroureter formation (Fig. 2A; Table S2A). Approximately 40% of *Pax2-cre/+;Fgfr1*$^{fl/+}$*;Fgfr2*$^{fl/+}$ (n=32) and 30% of *Pax2-cre/+;Fgfr1*$^{fl/fl}$*;Fgfr2*$^{fl/+}$ urogenital systems (n=11) presented with mild unilateral hydroureter, whereas *Pax2-cre/+;Fgfr1*$^{fl/+}$*;Fgfr2*$^{fl/fl}$ (n=26) and *Pax2-cre/+;Fgfr1*$^{fl/fl}$*;Fgfr2*$^{fl/fl}$ (n=8) urogenital systems had an increased occurrence (~85%) of strong bilateral hydroureter. In the last two genotypes, we detected one case each of ureter/kidney agenesis. Loss of both alleles of *Fgfr2* (*Pax2-cre/+;Fgfr1*$^{fl/+}$*;Fgfr2*$^{fl/fl}$; *Pax2-cre/+;Fgfr1*$^{fl/fl}$*;Fgfr2*$^{fl/fl}$) was additionally affected with uni- or bilateral dilatation of the epididymis, while kidney size and ureter length was strongly reduced in *Pax2-cre/+;Fgfr1*$^{fl/fl}$*;Fgfr2*$^{fl/fl}$ urogenital systems only (Fig. 2A; Table S2A). Histological analysis confirmed hydroureter formation upon loss of two or more alleles of *Fgfr1* and/or *Fgfr2*; however, this did not translate into hydronephrosis in any of the genotypes (Fig. 2B, Fig. S3A).

To test for patency of the ureter and its junctions, we injected ink into the renal pelvis of isolated urogenital systems and observed its flow to the bladder upon mild hydrostatic pressure. In most of the embryos with conditional loss of two or three alleles of *Fgfr1* and/or *Fgfr2* (*Pax2-cre/+;Fgfr1*$^{fl/+}$*;Fgfr2*$^{fl/+}$; *Pax2-cre/+;Fgfr1*$^{fl/fl}$*;Fgfr2*$^{fl/+}$; *Pax2-cre/+;Fgfr1*$^{fl/+}$*;Fgfr2*$^{fl/fl}$), the ureteric lumen was contiguous and the distal ureter inserted normally in the dorsal bladder neck. In 60% of *Pax2-cre/+;Fgfr1*$^{fl/fl}$*;Fgfr2*$^{fl/fl}$ urogenital systems (n=5), the ink did not reach the bladder, either due to insertion of the distal ureter into the urethra (1 out of 5) or due to ureteropelvic junction obstruction (n=2) (Table S2B). Histological analysis of the ureter-bladder connection of these specimens confirmed these findings (Fig. S3B). We conclude that loss of *Fgfr2* is associated with strong hydroureter formation. Additional loss of *Fgfr1* contributes to kidney hypoplasia and to increased physical obstruction along the ureter and its junctions.

We next used immunofluorescence analysis of marker proteins to judge cytodifferentiation of the epithelial and mesenchymal tissues of the ureter (Fig. 2C, columns 1-5). Expression of CDH1, a marker of the lateral-basal membrane of epithelial cells, was found in all mutants but the epithelium appeared mono-layered in mutants with loss of two alleles of *Fgfr2*. Expression of KRT5, ΔNP63 and UPK1B combinatorially marked B cells

Development (2022) 149, dev200021. doi:10.1242/dev.200021

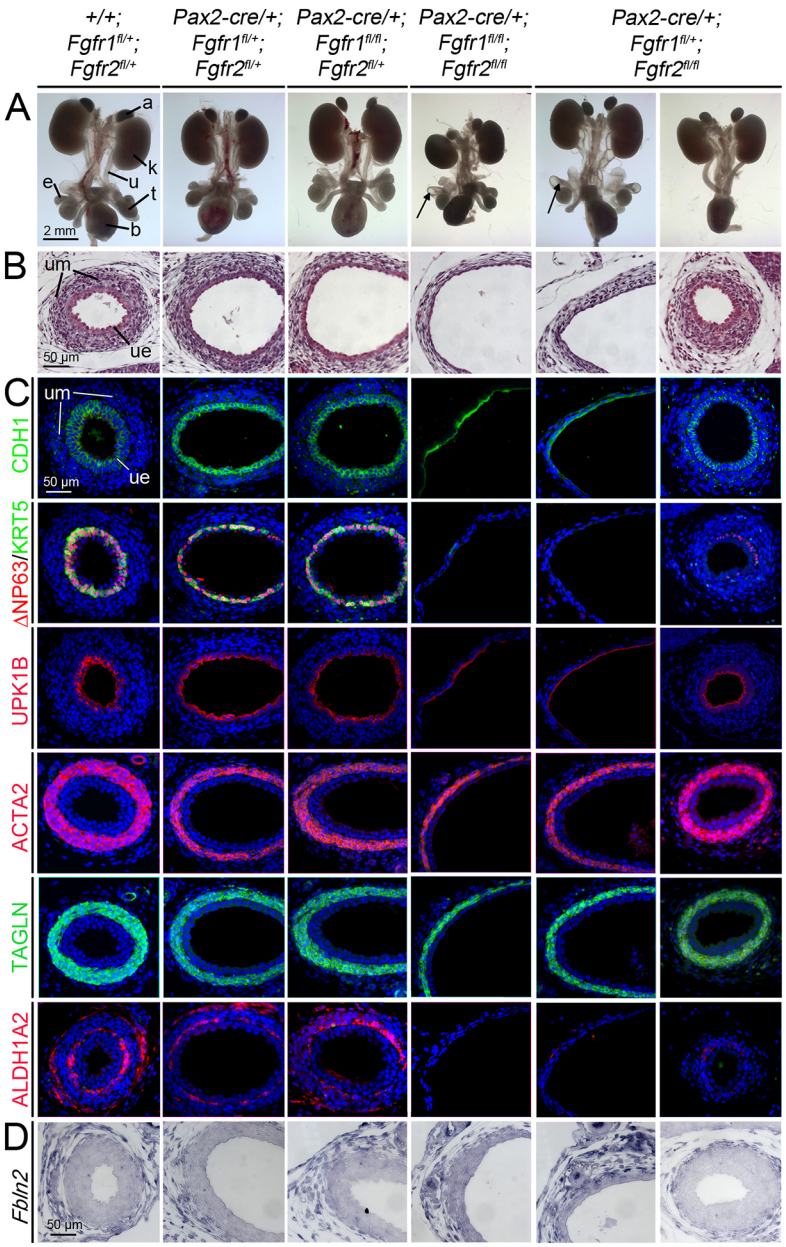

Fig. 2. Ureter anomalies in E18.5 embryos with conditional loss of *Fgfr1* and *Fgfr2* in the UE. (A) Morphology of whole urogenital systems of male embryos. Arrows indicate a dilated epididymis. For quantification data see Table S2A. (B) Hematoxylin and Eosin staining of transverse sections of the proximal ureter. (C,D) Analysis of marker expression for the basolateral membrane of epithelial cells (CDH1), for urothelial cell types [KRT5, ΔNP63 and UPK1B combinatorially mark B cells ($KRT5^{+}\Delta NP63^{+}UPK1B^{-}$), I cells ($KRT5^{-}\Delta NP63^{+}UPK1B^{low}$) and S cells ($KRT5^{-}\Delta NP63^{-}UPK1B^{high}$)], for SMCs (ACTA2 and TAGLN) and for the *lamina propria* (ALDH1A2) by immunofluorescence (C), and of the *tunica adventitia* marker *Fbln2* by *in situ* hybridization (D). Nuclei are counterstained with DAPI (C,D). $n \geq 3$ for all probes, assays and genotypes (B-D). a, adrenal; b, bladder; e, epididymis; k, kidney; t, testis; u, ureter; ue, ureteric epithelium; um, ureteric mesenchyme.

($KRT5^{+}\Delta NP63^{+}UPK1B^{-}$), I cells ($KRT5^{-}\Delta NP63^{+}UPK1B^{+}$) and S cells ($KRT5^{-}\Delta NP63^{-}UPK1B^{+}$) (Bohnenpoll et al., 2017c) in the control and in mutants with loss of one allele of *Fgfr2*. In mutants with a complete loss of *Fgfr2*, the mono-layered epithelium expressed the S-cell marker UPK1B, whereas KRT5- and ΔNP63-expressing B and I cells were largely absent. Expression of markers for SMCs (ACTA2 and TAGLN) and the *tunica adventitia* (*Fbln2*) occurred in the mesenchymal wall of all mutants; expression of a marker of the *lamina propria* (ALDH1A2) was absent in ureters with complete loss of *Fgfr2* function (Fig. 2C,D, columns 1-5).

Loss and/or reduction of ΔNP63, KRT5 and ALDH1A2 expression was also detected in a rare undilated *Pax2-cre/+;Fgfr1*$^{fl/+}$*;Fgfr2*$^{fl/fl}$ ureter, confirming the dilatation-independent nature of these changes (Fig. 2, column 6). We conclude that loss of *Fgfr2* in the UE compromises differentiation of I and B cells but also affects the development of *lamina propria* fibrocytes in the UM.

Early onset of cellular defects in *Fgfr2*-deficient ureters

To define both the onset as well as the progression of cellular defects in ureters with complete loss of *Fgfr2*, we analyzed earlier embryonic stages (Fig. 3). We used *Pax2-cre/+;Fgfr1*$^{fl/+}$*;Fgfr2*$^{fl/fl}$ (from now on termed *Fgfr2cKO*) embryos for this and all subsequent assays, as they exhibited the same ureteric cytodifferentiation defects as *Pax2-cre/+Fgfr1*$^{fl/fl}$*;Fgfr2*$^{fl/fl}$ embryos but presented in a normal Mendelian ratio. *Fgfr2cKO* ureters exhibited a clear histological division of the UM into an inner layer with rhomboid-shaped condensed cells and an outer layer with loosely organized fibroblast-like cells from E12.5 onwards, as in the control. However, both the UE and the UM were hypoplastic (Fig. 3A). The UE appeared less stratified at E14.5 and subsequent stages, and did not activate expression of ΔNP63 and KRT5. Expression of UPK1B occurred normally from E15.5 onwards. Expression of SMC markers was delayed by 1 day (Fig. 3B, Fig. S4 for higher magnification images of histological and CDH1 staining).

Development (2022) 149, dev200021. doi:10.1242/dev.200021

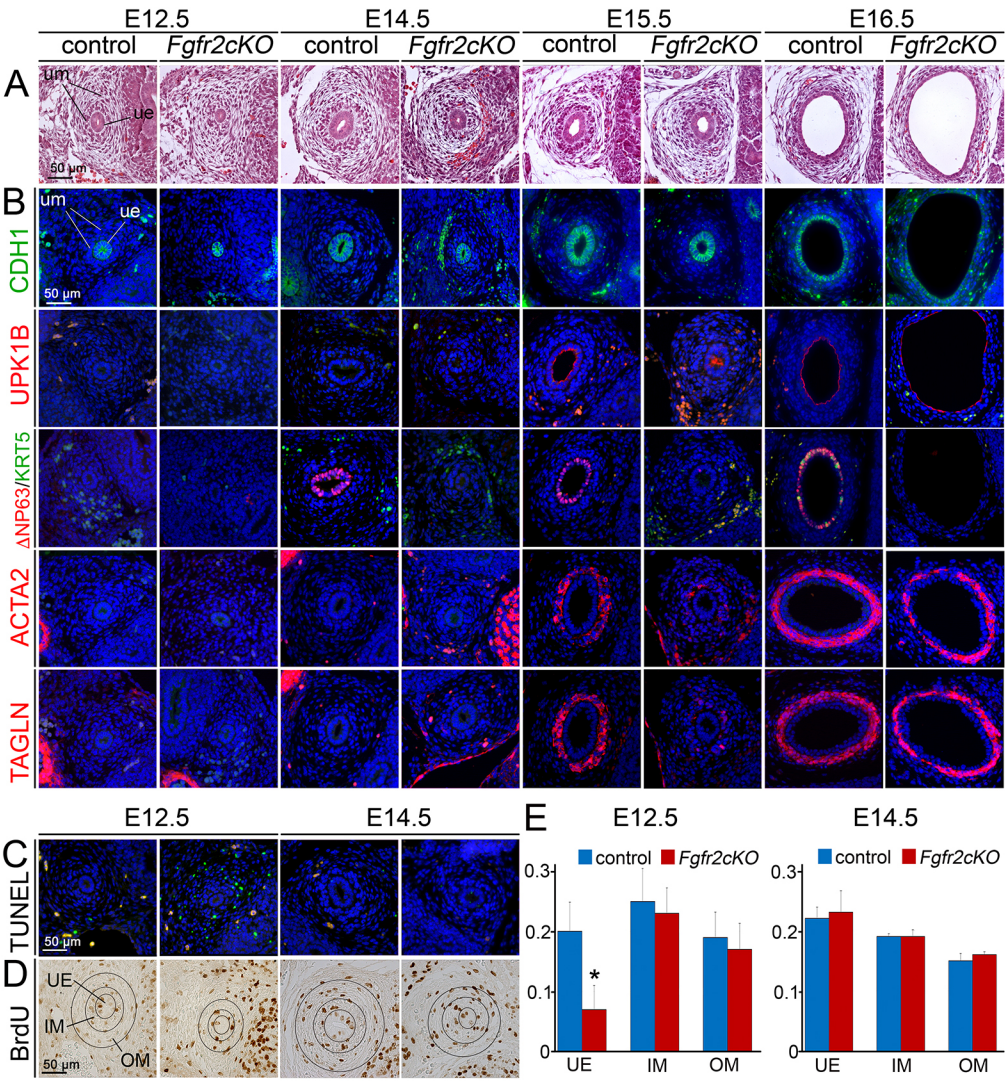

Fig. 3. Early onset of cellular changes in *Fgfr2cKO* ureters. (A) Hematoxylin and Eosin (HE) staining of transverse sections of the proximal region of the developing ureter at the indicated stages. (B) Analysis of marker expression for the epithelium (CDH1), for urothelial cell types (KRT5, ΔNP63 and UPK1B) and for SMCs (ACTA2 and TAGLN) in the developing ureter by immunofluorescence at the indicated stages. Nuclei are counterstained with DAPI (blue). (C) Immunofluorescence analysis (green) of apoptosis by the TUNEL assay on proximal ureter sections at E12.5 and E14.5. Nuclei are counterstained with DAPI (blue). Loss of *Fgfr2* in the UE leads to an increase in apoptosis in outer mesenchymal cells. (D) Determination of cellular proliferation by a BrdU incorporation assay on transverse sections of the proximal ureter at E12.5 and E14.5. Black circles mark the epithelium (UE) and the inner (IM) and outer (OM) mesenchymal compartments of the ureter in which proliferation was quantified. (E) Quantification of BrdU-positive cells (Table S3). E12.5, control versus mutant: UE, 0.2±0.05 versus 0.07±0.04, P=0.02; IM, 0.25±0.05 versus 0.23±0.04, P=0.42; OM, 0.19±0.04 versus 0.17±0.04, P=0.5. E14.5, control versus mutant: UE, 0.22±0.01 versus 0.23±0.03, P=0.56; IM, 0.19±0.01 versus 0.19±0.01, P=0.36; OM, 0.15±0.01 versus 0.16±0.01, P=0.09. Data are mean±s.d. *P<0.05; two-tailed Student's t-test. n≥3, for all probes, assays and genotypes. ue, ureteric epithelium; um, ureteric mesenchyme.

Given the obvious tissue hypoplasia in *Fgfr2cKO* ureters from E12.5 onwards, we analyzed whether changes in apoptosis and/or proliferation may be causative. In fact, the TUNEL assay detected apoptotic cells in the outer region of the UM at E12.5 (Fig. 3C). Moreover, the BrdU incorporation assay revealed strongly reduced proliferation in the UE of mutant embryos at this stage (Fig. 3D,E; Table S3). Hence, epithelial FGFR2 signaling plays a crucial role in epithelial proliferation, stratification and I-/B-cell differentiation, and (indirectly) in mesenchymal apoptosis and differentiation.

Reduced activity of a *Shh-Foxf1-Bmp4* module in *Fgfr2cKO* ureters

We next performed transcriptional profiling by microarray analysis of E13.5 *Fgfr2cKO* and control ureters to identify molecular changes that may underlie the cellular defects in these mutants. Using an intensity threshold of 100 and fold changes of at least 1.5, we identified 97 genes that were consistently upregulated and 49 genes that were downregulated in *Fgfr2cKO* ureters (Fig. 4A; Tables S4 and S5). Functional annotation by DAVID did not find enrichment of meaningful terms in the list of upregulated genes (Table S6). However, in the pool of downregulated genes terms associated with SHH/SMO activity and AP1 signaling were over-represented (Table S7).

In fact, among the most downregulated genes were *Hhip*, *Ptch1* and *Foxf1*, which have previously been found to depend on SHH signaling in the ureter (Bohnenpoll et al., 2017c), *Shh* itself and AP1/immediate early genes (*Fosb*, *Egr1*, *Fos* and *Egr2*). Moreover, *Hoxb8*, a gene linked to proliferation control (Guo et al., 2019; Wang et al., 2019), was strongly reduced as was *Aldh1a3*, a gene encoding an RA-synthesizing enzyme, and *Elf5* (Fig. 4A), an epithelial target of RA signaling in the ureter (Bohnenpoll et al., 2017b). *Spry1* and *Spry2*, direct targets of FGF signaling (Hanafusa et al., 2002), were reduced confirming our previous analysis (Fig. S2).

We used *in situ* hybridization analysis to validate these changes in E12.5 and E14.5 *Fgfr2cKO* ureters. We detected reduced expression of *Hoxb8*, *Aldh1a3* and *Elf5* in the UE at E12.5 (Fig. 4B,C). Expression of *Shh* was strongly reduced in the UE, as was expression of *Ptch1* and *Foxf1* in the UM at E12.5 and E14.5 (Fig. 4D). Expression of *Fosb*, *Egr1* and *Fos* was not detected in the control or was unchanged in the mutant (Fig. S5).

Given the strong downregulation of the *Shh-Foxf1* axis, we also analyzed expression of the effector gene of this pathway: *Bmp4* (−1.2 in the microarray) (Mamo et al., 2017). *Bmp4* expression was clearly reduced in the UM both at E12.5 and E14.5. Moreover, expression of Id genes (*Id2*, *Id3* and *Id4*), direct transcriptional

Development (2022) 149, dev200021. doi:10.1242/dev.200021

A

Gene	avgFC
Hoxb8	**-3.1**
Nhlrc4	-2.4
9030625G05Rik	-2.4
Fosb	-2.3
Gsta2	-2.3
Hhip	-2.2
Calcr	-2.2
Gm10639	-2.1
TC1605611	-2.1
Mapk4	-2.0
A930017K11Rik	-2.0
Prr7	-1.9
Mia	-1.9
Fos	-1.9
Rbm47	-1.9
Mllt3	-1.9
Egr1	-1.9
Sprr2f	-1.9
Espn	-1.9
Frmd5	-1.9

Gene	avgFC
Hs3st6	-1.9
Fam150b	-1.8
Ldoc1	-1.8
Degs2	-1.8
Egr2	-1.8
Sel1l3	-1.8
Kcnj16	-1.8
Tfap2b	-1.8
Srrm2	-1.8
Arhgef38	-1.8
Aldh1a3	**-1.7**
Gprc5b	-1.7
Tmem229a	-1.7
A4galt	-1.7
Shh	**-1.7**
E330013P04R	-1.7
Foxf1	**-1.7**
Clu	-1.7
Map7	-1.7
Tfrc	-1.6

Gene	avgFC
Gabbr2	-1.6
Dclk3	-1.6
Ccdc172	-1.6
Afm	-1.6
A_55_P2028852	-1.6
Elf5	**-1.6**
Atp1b1	-1.6
Nr1h5	-1.5
Iqck	-1.5
Ptch1	**-2.0 (-1.3/-2.7)**
Bmp4	**-1.2 (1.0/-1.4)**
Aldh1a2	-1.3 (-1.2/-1.3)
Rarb	1 (-1.1/1.1)
Wnt7b	**-1.6 (-1.4/-1.7)**
Wnt9b	-1.4 (-1.4/-1.4)
Axin2	**-1.2 (1.0/-1.5)**
Spry1	**-1.8 (-1.4/-2.2)**
Spry2	**-1.8 (-1.4/-2.2)**

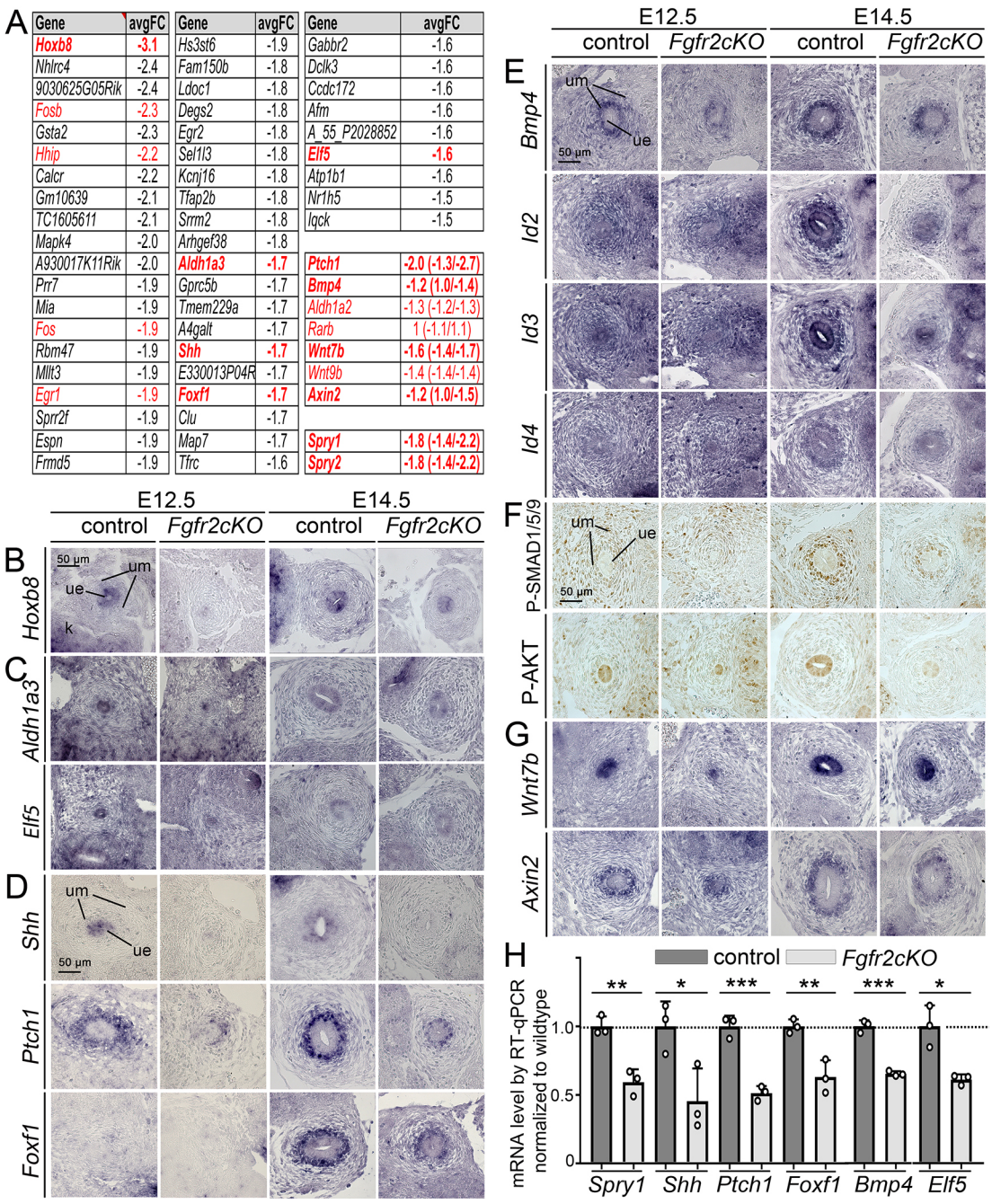

Fig. 4. The *Shh-Foxf1-Bmp4* signaling axis is compromised in *Fgfr2cKO* ureters. (A) Table of transcripts with reduced expression in microarrays of E13.5 *Fgfr2cKO* ureters. Shown are average fold changes (avgFC). Genes in red are validated by *in situ* hybridization, the ones in bold show reduced expression in this assay. All genes in the lower right column did not fulfill the initial filter criteria but were additionally validated. (B-E,G) *In situ* hybridization analysis on transverse sections of the proximal ureter of E12.5 and E14.5 control and *Fgfr2cKO* embryos for expression of *Hoxb8* (B), of an epithelial RA component (*Aldh1a3*) and target (*Elf5*) (C), of components and targets of SHH signaling (*Shh*, *Ptch1* and *Foxf1*) (D), of *Bmp4* and direct transcriptional targets of its activity (*Id2*, *Id3* and *Id4*) (E), and of an epithelial WNT ligand gene (*Wnt7b*) and a target of WNT signaling (*Axin2*) (G). (F) Immunohistochemical detection of activated, i.e. phosphorylated, forms of cytoplasmic effectors of BMP4 signaling (P-SMAD1/5/9 and P-AKT) on transverse sections of the proximal ureter of E12.5 and E14.5 control and *Fgfr2cKO* embryos. $n \geq 3$ for all probes, genotypes and stages. (H) RT-qPCR results of expression of selected signaling components and targets in three independent total RNA pools of E14.5 *Fgfr2cKO* and control ureters. For statistical values, see Table S8. Differences were considered significant (*$P<0.05$), highly significant (**$P \leq 0.01$) or extremely significant (***$P \leq 0.001$); two-tailed Student's *t*-test. Data are mean±s.d. k, kidney; ue, ureteric epithelium; um, ureteric mesenchyme.

targets of BMP signaling (Hollnagel et al., 1999; Liu and Harland, 2003), was reduced both in the UE and UM of *Fgfr2cKO* embryos at E14.5 (Fig. 4E). As BMP4 signaling is mediated by different cytoplasmic effector proteins in the developing ureter (Mamo et al., 2017), we analyzed their activated, i.e. phosphorylated, forms by immunohistochemistry. We found reduced expression of P-SMAD1/5/9 in the UM, and of P-AKT in the UE at E14.5, while P-ERK1/2 and P-P38 expression was unaffected (Fig. 4F; Fig. S6).

In agreement with the microarray data, other signaling systems involved in ureteric proliferation and differentiation were either not

Development (2022) 149, dev200021. doi:10.1242/dev.200021

or only marginally affected. Expression of mesenchymal RA signaling components (*Aldh1a2*) and targets (*Rarb*) (Mendelsohn et al., 1991) was unchanged (Fig. S5). Expression of *Wnt7b* was weakly reduced in the UE at E12.5; *Wnt9b* expression in the UE was normal; expression of *Axin2* was weakly reduced in the UM (Fig. 4G, Fig. S5).

Finally, RT-qPCR analysis confirmed significantly reduced expression of *Spry1*, *Shh*, *Ptch1*, *Foxf1*, *Bmp4* and *Elf5* in E14.5 *Fgfr2cKO* ureters (Fig. 4H; Table S8). We conclude that the *Shh-Foxf1-Bmp4* axis is strongly affected by loss of epithelial *Fgfr2* in the early ureter, whereas RA and WNT signaling are only partly and weakly compromised.

SHH and BMP4 signaling mediates FGFR2 function

To test the individual contribution of reduced SHH, BMP4, RA and WNT signaling activity to the proliferation and cytodifferentiation defects of *Fgfr2cKO* ureters, we performed pharmacological pathway rescue experiments in *ex vivo* cultures (Fig. 5). As we were not able to confirm expression (changes) of AP1 components and targets in the UM of mutants (Fig. S5), we excluded this pathway from further investigation.

Fgfr2cKO ureters explanted at E13.5 and cultured for 4 days in minimal medium (DMEM only) exhibited a short ureter with epithelial tissue hypoplasia. Moreover, the ratio of $\Delta NP63^{+}$ to $CDH1^{+}$ cells dropped to around 50% (control: 90%), the thickness of the SMC layer (marked by TAGLN) was reduced and expression of the *lamina propria* marker ALDH1A2 was nearly absent, highly reminiscent of the changes observed *in vivo*. Addition of 2 µM of the SHH signaling/SMO agonist purmorphamine (Li et al., 2008) or of 100 ng/ml BMP4 increased the percentage of $\Delta NP63^{+}$ cells in *Fgfr2cKO* ureter explants almost to control level and rescued epithelial hypoplasia. In the case of reactivation of the SHH signaling pathway, mesenchymal aspects of the *Fgfr2cKO* phenotype were also rescued: expression of ALDH1A2 was restored as was the thickness of the SMC layer. Addition of BMP4 rescued the mesenchymal phenotype partly. Addition of 1 µM RA enhanced the loss of $\Delta NP63^{+}$ and $ALDH1A2^{+}$ cells, and did not rescue the tissue hypoplasia of the mutant ureter. The WNT agonist BIO (Sato et al., 2004) rescued the epithelial hypoplasia but left all other parameters in *Fgfr2cKO* ureters unaffected (Fig. 5; Table S9). Hence, SHH and BMP4 signaling are functional mediators of FGFR2 activity in the UE.

Inhibition of SHH or BMP4 signaling dose-dependently compromises epithelial and mesenchymal differentiation in the ureter

Previous work has shown that the genetic ablation of SHH and BMP4 signaling leads to tissue hypoplasia and a complete lack of cytodifferentiation (Bohnenpoll et al., 2017c; Mamo et al., 2017). To explore the consequences of a partial reduction of these signaling activities for ureter development, we explanted E13.5 wild-type ureters and cultured them for 4 days in DMEM supplemented with increasing concentrations of the SMO antagonist cyclopamine (Chen et al., 2002; Cooper et al., 1998) or noggin (NOG), which sequesters BMP4 from its receptor (Zimmerman et al., 1996). In both cases, we detected a dose-dependent decrease of stratification and of $\Delta NP63^{+}$ cells, a reciprocal increase of luminal $\Delta NP63^{-}$ cells that were lined by UPK expression at low and medium doses, and an ablation (cyclopamine) or reduction (NOG) of the SMC layer. At the highest doses of NOG, UPK expression was partially reduced. Expression of ALDH1A2 was strongly affected by mild reduction of SHH signaling, whereas reduction of BMP4 signaling had a weaker but dose-dependent effect (Fig. 6A-E; Fig. S7 for higher magnification images of histological and CDH1 staining; Table S10). We conclude that reduction of SHH or BMP4 signaling largely recapitulates the phenotypic changes in *Fgfr2cKO* ureters.

DISCUSSION

Epithelial FGFR2 signaling controls multiple cellular programs in both the mesenchymal and epithelial compartment of the ureter

Previous work described the role of FGFR signaling in the development of numerous components of the urinary system, but its role(s) in ureter development has remained unexplored (Walker et al., 2016). Based on their expression in the early UE, we used a conditional gene targeting experiment to analyze the specific function of *Fgfr1* and *Fgfr2* in this tissue. Our phenotypic characterization of compound and double mutants revealed that FGFR2 function maintains the structural integrity of the ureter by controlling different cellular programs in both the epithelial and mesenchymal tissue compartment of this organ.

Owing to our breeding strategy, we recovered only *Fgfr1-Fgfr2* compound mutants for phenotypic analysis. Although we cannot formally exclude a (minor) contribution of heterozygous loss of *Fgfr1* to the observed phenotypic changes of the ureter in embryos with homozygous loss of *Fgfr2*, we are convinced that control of early ureter development is exerted almost exclusively by FGFR2. First, *Fgfr2* is much more strongly expressed than *Fgfr1* in the UE from E12.5 to E14.5. Second, complete loss of *Fgfr1* with combined loss of one allele of *Fgfr2* did not result in changes in FGF signaling, i.e. *Spry1* and *Spry2* expression, in the UE, whereas complete loss of *Fgfr2* did. Third, complete loss of *Fgfr2* but not of *Fgfr1* resulted in severe ureteric cytodifferentiation defects. Fourth, FGF7 and FGF10, the two ligands with expression in the UM, predominantly signal through the epithelial isoform of FGFR2 (Igarashi et al., 1998; Jans, 1994; Ornitz and Itoh, 2015), whereas specific expression of FGF ligands that preferentially signal through FGFR1 was not detected in the early ureter. Fifth, previous studies using a *Hoxb7cre* line for recombination in the ureteric bud lineage did not detect defects in the urogenital system of *Hoxb7cre/+;Fgfr1*$^{fl/fl}$ embryos, whereas *Hoxb7cre/+;Fgfr2*$^{fl/fl}$ embryos exhibited renal hypo(dys)plasia due to reduced branching morphogenesis, and thinning of the early ureter and hydroureter, which are highly reminiscent of the phenotypic changes observed in our *Pax2-cre/+;Fgfr1*$^{fl/+}$*;Fgfr2*$^{fl/fl}$ embryos (Sims-Lucas et al., 2011; Zhao et al., 2004).

Although we detected embryonic lethality in our compound mutants, *Hoxb7cre/+;Fgfr1*$^{fl/fl}$, *Hoxb7cre/+;Fgfr2*$^{fl/fl}$ and *Hoxb7cre/+;Fgfr1*$^{fl/fl}$*;Fgfr2*$^{fl/fl}$ mice exhibited a normal Mendelian distribution at embryonic and adult stages (Sims-Lucas et al., 2011; Zhao et al., 2004). The *Pax2-cre* line used in our conditional gene targeting experiments also recombines outside the nephric duct epithelium (and its derivatives), particularly strongly in the midbrain-hindbrain region and the branchial arches at E9.5 (Kuschert et al., 2001). These expression domains are likely to give rise to vessels in the brain but also to the second heart field from which the atria, the right ventricle and the outflow region are derived (Kelly et al., 2001; Mjaatvedt et al., 2001). Given the known role of FGF signaling in the second heart field region and in vessel development (Park et al., 2008; Yang et al., 2015), deletion of *Fgfr1* and/or *Fgfr2* might contribute to embryonic lethality due to cardiac/circulatory insufficiency.

The study by Zhao et al. characterized the function of *Fgfr2* in renal development, but it did not explain the thinning of the early

Development (2022) 149, dev200021. doi:10.1242/dev.200021

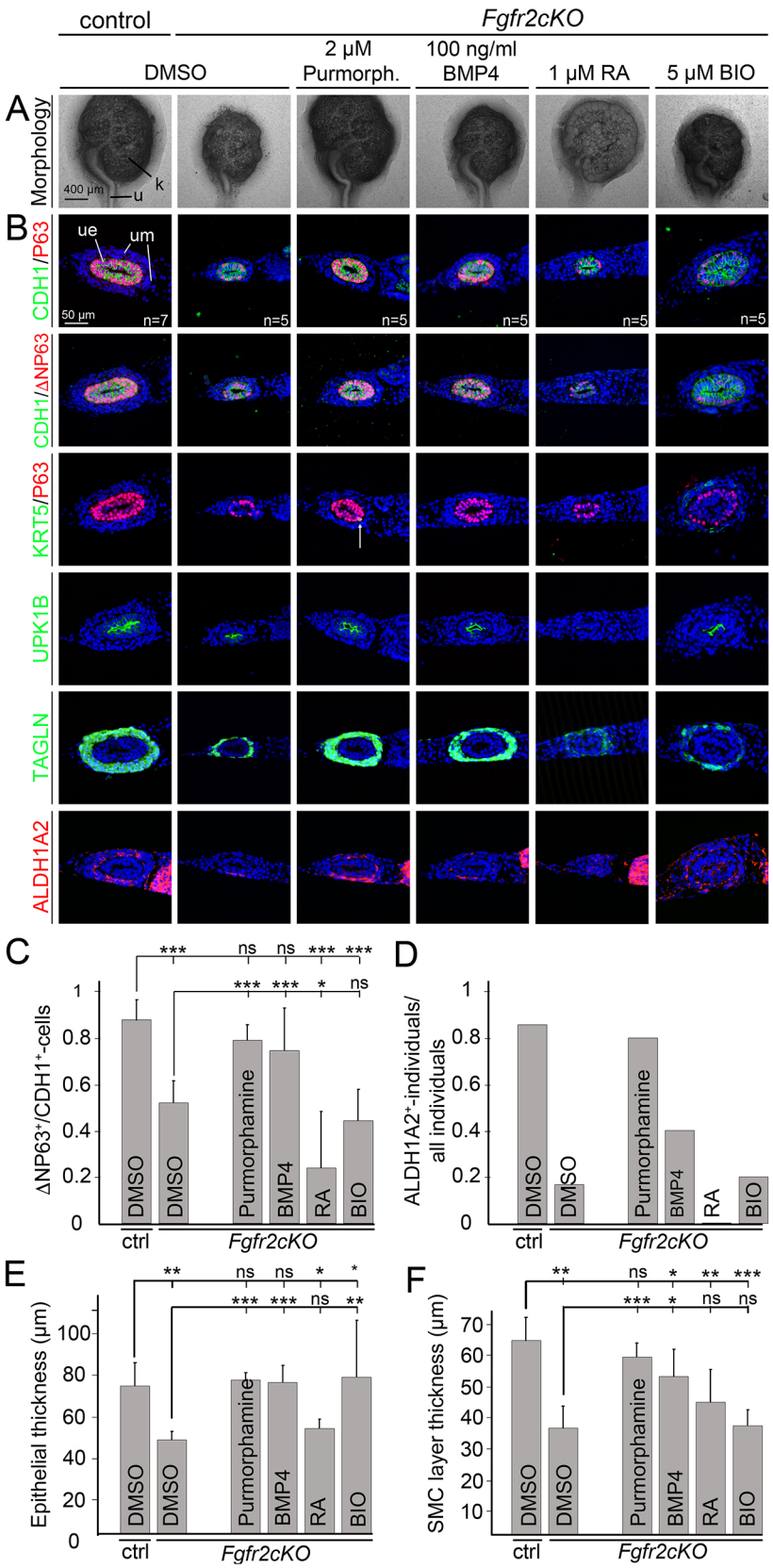

Fig. 5. Restoration of SHH or BMP4 signaling rescues epithelial and mesenchymal proliferation and differentiation defects in *Fgfr2cKO* ureters in explant cultures. E13.5 control and *Fgfr2cKO* ureters were cultured for 4 days in DMEM supplemented with DMSO (as a control), 2 µM of the SHH signaling agonist purmorphamine (Purmorph.), 100 ng/ml BMP4, 1 µM RA or 5 µM WNT signaling activator BIO. (A) Bright-field images of kidney (k) and ureter (u) explants after 4 days of culture. (B) Immunofluorescence analysis on transverse sections of the proximal ureter for expression of markers for the epithelium (CDH1), urothelium (KRT5, ΔNP63 and UPK1B), SMCs (TAGLN) and *lamina propria* (ALDH1A2). The arrow (row 3, column 3) points to a single KRT5$^+$ cell. *n*=7 for the control; *n*=5 for the mutant for all assays (B-F). ue, ureteric epithelium; um, ureteric mesenchyme. (C-F) Quantification on transverse sections of the proximal ureter of the ratio of ΔNP63$^+$ to CDH1$^+$ epithelial cells (C), of the percentage of sections with ALDH1A2$^+$ cells (D), of the epithelial thickness (E) and of the SMC layer thickness (F). For statistical values, see Table S9. Differences were considered non-significant (ns; $P>0.05$), significant (*$P<0.05$), highly significant (**$P\leq0.01$) or extremely significant (***$P\leq0.001$); two-tailed Student's *t*-test. The upper lines refer to the statistical difference compared with the DMSO-treated control (ctrl), the lower lines refer to DMSO-treated *Fgfr2cKO* ureter explants. Data are mean±s.d.

ureter and hydroureter formation in these mice (Zhao et al., 2004). Our study shows that these defects relate to an independent function of FGFR2 signaling in the development of the distal aspect of the ureteric bud. Epithelial *Fgfr2* was required for proliferation, stratification and I-/B-cell differentiation in the UE but its loss also had an impact on apoptosis, and SMC as well as *lamina propria* differentiation in the UM. Although work in the bladder assigned FGF7 and FGF10 a role as mitogens for I cells (Bagai et al., 2002;

Development (2022) 149, dev200021. doi:10.1242/dev.200021

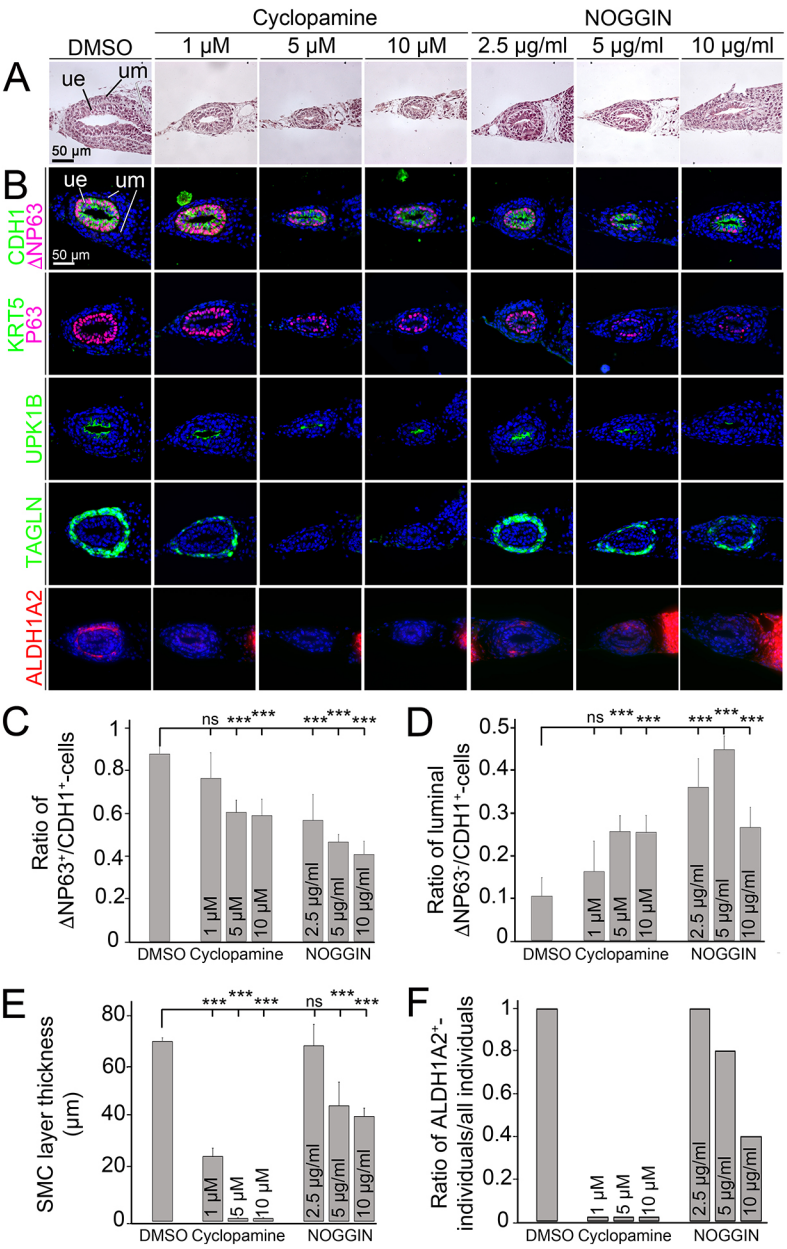

Fig. 6. Inhibition of SHH or BMP4 signaling dose-dependently compromises epithelial and mesenchymal differentiation in the ureter. E13.5 wild-type ureters were cultured for 4 days with increasing concentrations of the SHH signaling inhibitor cyclopamine or the BMP4 antagonist noggin (NOG). (A,B) Transverse sections of the proximal region of E13.5 ureters cultured for 4 days under the indicated conditions were analyzed by Hematoxylin and Eosin staining (A), and by (co-)immunofluorescence analysis for expression of the epithelial marker CDH1 with ΔNP63, the B-cell marker KRT5 with P63, the S-cell marker UPK1B and the SMC marker TAGLN (B). ue, ureteric epithelium; um, ureteric mesenchyme. (C-F) Transverse sections of the proximal ureter cultured in the presence of increasing concentrations of cyclopamine or NOG were quantified for the ratio of $\Delta NP63^{+}$ cells to $CDH1^{+}$ cells (C), for the ratio of $\Delta NP63^{-}$ luminal cells to $CDH1^{+}$ cells (D), for the thickness of the SMC layer (E), and for the ratio of $ALDH1A2^{+}$ individuals to all individuals (F) compared with the DMSO control. For statistical values, see Table S10. Differences were considered non-significant (ns) with $P>0.05$ or extremely significant (***$P\leq0.001$); two-tailed Student's *t*-test. $n\geq5$ for all assays. Data are mean±s.d.

Tash et al., 2001; Zhang et al., 2006), our findings indicate a broader function for epithelial FGFR signaling – using a relay system – to coordinate the development of both tissue compartments in the early ureter.

Our ink injection experiments revealed that in *Fgfr2cKO* urogenital systems physical obstruction occurs only in 20% of the specimens, indicating that delayed SMC differentiation contributes or causes hydroureter formation, as observed in other mouse models (Weiss et al., 2019). Luminal occlusion in distal ureter regions due to epithelial hypoplasia and/or distal ureter maturation defects due to delayed ureter budding may contribute to this defect, as reported for *Hoxb7-cre/+;Fgfr2*$^{fl/fl}$ mice (Sims-Lucas et al., 2011; Zhao et al., 2004). Our *Fgfr1/Fgfr2* double mutants exhibited an increased incidence of hydroureter formation due to ureteropelvic junction obstruction, a blind-ending distal ureter and ectopic urethral connectivity. They also showed strong renal and ureter hypoplasia. We assume that these defects reflect the combined function of *Fgfr1* and *Fgfr2* in UB formation, and branching morphogenesis of the collecting duct system from the proximal UB tip region, as previously reported (Sims-Lucas et al., 2011; Zhao et al., 2004).

Shh is a functional target of FGFR2 in the UE

Fgfr2cKO ureters exhibit a spectrum of phenotypic changes in both the epithelial and mesenchymal compartment that are similar in nature but reduced in severity compared with those seen when the SHH-FOXF1-BMP4 signaling axis is lost. Moreover, the temporal window of epithelial FGFR2 signaling activity aligns with the expression profile of *Shh* and *Bmp4* in the ureter; both are strongly downregulated after E14.5 (Bohnenpoll et al., 2017c; Mamo et al., 2017; Yu et al., 2002). Expression of *Shh* as well as of *Ptch1*, *Foxf1* and *Bmp4*, which represent the *Shh* effector level, was reduced in *Fgfr2cKO* ureters. Activation of SHH/SMO signaling by purmorphamine and addition of BMP4 largely rescued the proliferation and differentiation defects in *Fgfr2cKO* ureters. Finally, reduction of SHH and BMP4 signaling in wild-type ureters recapitulated the phenotypic changes observed in *Fgfr2cKO* ureters

Development (2022) 149, dev200021. doi:10.1242/dev.200021

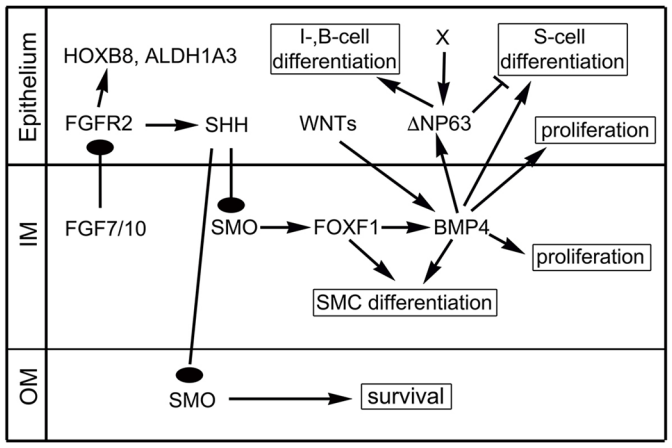

Fig. 7. Model of FGFR2 signaling function in the early ureter. FGFR2 signaling in the UE augments *Shh* expression and, hence, the SHH-FOXF1-BMP4 signaling axis in the UM, which accounts for mesenchymal and epithelial proliferation and differentiation (processes are boxed). FGFR2 may activate expression of additional genes in the UE (*Hoxb8* and *Aldh1a3*) independently of *Shh*. Factor X provides an unknown input for ΔNP63 expression. Arrows indicate activating interactions, dots indicate ligand receptor interaction. IM, inner mesenchyme; OM, outer mesenchyme.

in a dose-dependent manner. Together, this provides compelling evidence that FGFs act via FGFR2 to enhance *Shh* expression and consequently SHH-FOXF1-BMP4 activity in the early ureter (Fig. 7).

It is important to note that the FGF7/10-FGFR2-SHH-BMP4 signaling axis has previously been characterized in the early development of other organs, including the urethra, the limb, the palate and the eyelid (Huang et al., 2009; Petiot et al., 2005; Revest et al., 2001; Rice et al., 2004). The primordia of all of these organs, as well as of the ureter and bladder are characterized by a composite design with epithelial and mesenchymal tissue compartments. The coordinated development of these compartments is assured by reciprocal signaling systems in which the FGF7/10-FGFR2-SHH-BMP4 module seems of outstanding relevance.

Our microarray analysis identified *Hoxb8* as the most downregulated gene in the *Fgfr2cKO* ureter. As *Hoxb8* has been implicated in proliferation control (Guo et al., 2019; Wang et al., 2019), its reduced expression in the UE may contribute to urothelial hypoplasia. Importantly, *Hoxb8* does not depend on SHH signaling in the ureter (Bohnenpoll et al., 2017c), and can be ectopically induced in neural tissues of the chick by FGF treatment (Bel-Vialar et al., 2002). This suggests that FGFR2 signaling regulates a set of genes independently of the SHH-FOXF1-BMP4 signaling axis.

Urothelial cell fates may depend on gradients of BMP4

Fgfr2cKO ureters displayed a mono-layered urothelium consisting of S cells. This phenotype is highly reminiscent of that seen in the bladder and ureters of mice with conditional loss of ΔNP63 in the respective epithelial primordium (Cheng et al., 2006; Pignon et al., 2013; Weiss et al., 2013). Failure to activate ΔNP63 in *Fgfr2cKO* ureters, therefore, likely accounts for the lack of stratification and B-cell differentiation in the mutant urothelium.

Expression and lineage tracing analysis uncovered that S and B cells are terminally differentiated cell types that arise from a common progenitor by an I-cell intermediate. The I cells were recognized as $\Delta NP63^{+}$ cells lacking high expression of UPKs and KRT5 (Bohnenpoll et al., 2017a; Gandhi et al., 2013). Differentiation of S cells in absence of ΔNP63 shows that stratification is not a prerequisite for S-cell differentiation, and suggests that S-cell differentiation is normally inhibited by ΔNP63 in I cells.

Mice with conditional loss of *Smo* or *Bmp4* in the UM do not activate ΔNP63 in the urothelium, and lack stratification and B- and S-cell differentiation (Bohnenpoll et al., 2017c; Mamo et al., 2017). In *Fgfr2cKO* ureters, *Shh* and, consequently, *Bmp4* expression is reduced but not lost, suggesting that ΔNP63 expression and stratification requires higher levels of SHH and BMP4 signaling than S-cell differentiation. This notion is supported by the restoration of ΔNP63 expression in *Fgfr2cKO* ureters by purmorphamine and BMP4 treatment, on the one hand, and a relatively higher decrease in I cells compared with S cells by increasing doses of cyclopamine and NOG in wild-type ureters, on the other hand. Administration of BMP4 to early kidney explants leads to UPK expression in collecting duct cells (Mills et al., 2017; Wang et al., 2009), indicating that BMP4 is required and sufficient to activate S-cell differentiation. It is conceivable that ectopic induction of I-cell differentiation and of ΔNP63 expression, respectively, require higher levels of BMP4 and/or additional positive signals, similar to the situation in other epithelia (Terakawa et al., 2016). Alternatively, concurrent repression of an inhibitor may allow induction of ΔNP63.

Interestingly, the epithelium covering the renal papilla is monolayered and consists of S cells only. It is conceivable that out of the reach of FGF7/FGF10 signals, the SHH-BMP4 axis is not sufficiently augmented to activate ΔNP63 and to drive stratification at this site.

FGFR2 signaling and urothelial regeneration

Our expression analysis showed that *Fgfr2* is strongly downregulated after E14.5, excluding a role for FGFR2 signaling in later (fetal) development and homeostasis. This is consistent with the mature urothelium being quiescent. However, under conditions of injury or infection, proliferation of I cells and differentiation into S and B cells resume to repair the urothelium within days. Interestingly, recent reports revealed that FGF7 and FGFR2 function is reused in this program (Girshovich et al., 2012; Narla et al., 2020). Whether an FGF7-FGFR2 module employs the SHH-BMP4 signaling axis in regeneration similar to the embryonic situation is an interesting question for future research.

MATERIALS AND METHODS

Mice

Mice with *loxP* sites flanking exon 4 of the *Fgfr1* locus (*Fgfr1*$^{tm5.1Sor}$; synonym: *Fgfr1*^{fl}) (Hoch and Soriano, 2006) and mice with *loxP* sites flanking exons 7 to 10 of the *Fgfr2* locus (*Fgfr2*^{tm1Dor}; synonym: *Fgfr2*^{fl}) (Yu et al., 2003) were obtained from the Jackson Laboratory. *Tg(Pax2-cre)1AKis* (synonym: *Pax2-cre*) mice were previously generated in the lab (Bohnenpoll et al., 2017a; Trowe et al., 2011). All mice were maintained on a NMRI outbred background. Embryos for expression analysis of genes encoding FGF signaling components as well as for loss-of-function experiments were obtained from NMRI mice; embryos for phenotype analysis were generated by mating *Pax2-cre/+;Fgfr1*$^{fl/+}$*;Fgfr2*$^{fl/+}$ males with *Fgfr1*$^{fl/fl}$*;Fgfr2*$^{fl/fl}$ females. *Cre*-negative littermates were used as controls. For timed pregnancies, vaginal plugs detected in the morning after mating were designated as embryonic day (E) 0.5 at noon. Urogenital systems and embryos were dissected in PBS, fixed in 4% paraformaldehyde (PFA) in PBS and stored in methanol at −20°C. For genotyping by PCR, genomic DNA prepared from yolk sacs or ear clip biopsies was used.

Mice were housed in rooms with controlled light and temperature. The experiments were carried out in accordance with the German Animal Welfare Legislation and approved by the local Institutional Animal Care and

Development (2022) 149, dev200021. doi:10.1242/dev.200021

Research Advisory Committee and permitted by the Lower Saxony State Office for Consumer Protection and Food Safety (AZ 33.12-42502-04-13/1356, AZ42500/1H).

Organ cultures

Ureters for explant cultures were dissected in L-15 Leibovitz medium (F1315, Biochrom), explanted on 0.4 µm polyester membrane Transwell supports (657610, Greiner Bio-One) and cultured at the air-liquid interface with DMEM/F12 (21331020, Gibco) supplemented with 1×penicillin/streptomycin (15140122, Gibco), 1×NEAA (11140035, Gibco), 1×pyruvate (11360070, Gibco) and 1×glutamax (35050038, Gibco) in a humidified incubator with 5% CO_2 at 37°C. Pathway activating components were dissolved as follows: recombinant human BMP4 (100 ng/µl in 4 mM HCl/0.1% BSA; PHP171, Abd Serotec), purmorphamine (2 µM in DMSO; 540220, Merck), retinoic acid (RA; 1 µM in DMSO; R2625, Sigma-Aldrich), 6-bromoindirubin-3′-oxime (BIO, 5 µM in DMSO; S7198, Selleckchem), cyclopamine (1-10 µM in DMF; S11465, Selleckchem) and NOG (2.5-10 µg/ml in double distilled H_2O; Z0320525, Genescript). Medium containing DMSO or components was refreshed every second day.

Morphological, histological and immunohistochemical analyses

Kidney size and ureter length was measured using the segmented line tool from Image J (Schindelin et al., 2012). Ureter length was measured from the pelvic region to the bladder insertion site. Kidney size was calculated by measuring the cranial to caudal length and the medial to lateral width.

Embryos, urogenital systems and ureter explants were fixed in 4% PFA, embedded in paraffin wax and sectioned at 5 µm. Sections were stained with Hematoxylin and Eosin according to standard procedures.

Immunofluorescence staining as well as immunohistochemistry was performed on 5 µm paraffin wax-embedded sections using the following primary antibodies and dilutions: monoclonal mouse-anti-BrdU (1:250; WH0007348M2, Sigma-Aldrich) polyclonal rabbit-anti-KRT5 (1:200; PRB-160P, BioLegend), polyclonal rabbit-anti-ΔNP63 (1:100; clone Poly6190, 619001, BioLegend), monoclonal mouse-anti-P63 (1:200; clone 4A4, ab735, Abcam), monoclonal mouse-anti-UPK1B (1:200; clone1E1, WH0007348M2, Sigma-Aldrich), polyclonal rabbit-anti-TAGLN (1:200; ab14106, Abcam), polyclonal mouse-anti-ACTA2 (1:200; A5228; clone 1A4; Merck), polyclonal rabbit-anti-ALDH1A2 (1:200; ab75674, Abcam), polyclonal rabbit-anti-CDH1 (1:200, a kind gift from Dr R. Kemler, MPI, Freiburg, Germany), monoclonal rabbit-anti-P-SMAD1/5/9 (1:100; 13280, Cell Signaling), monoclonal rabbit-anti-P-P38 MAPK (1:100; 4631, Cell Signaling), monoclonal rabbit-anti-P-AKT (1:100; 9271, Cell Signaling) and monoclonal rabbit-anti-P-ERK1/2 (1:100; 9102, Cell Signaling). Fluorescent staining was performed using the following secondary antibodies: biotinylated goat-anti-rabbit IgG (1:200; 111065033, Dianova), biotinylated goat-anti-mouse IgG (1:200; 115-065-166, Jackson ImmunoResearch), Alexa488-conjugated goat-anti-rabbit IgG (1:400; A11034, Molecular Probes) and Alexa555-conjugated goat-anti-mouse IgG (1:400; A21422, Molecular Probes). The signals of ΔNP63, P63 and ALDH1A2 were amplified using the Tyramide Signal Amplification system (NEL702001KT, Perkin Elmer). For co-staining with primary antibodies of the same host (ΔNP63 and KRT5 or CDH1), the staining was performed sequentially and the epitope of the first antibody was blocked with goat-anti-rabbit FAB fragment (1:50; 111007003, Dianova). The signals of P-SMAD1/5/9, P-AKT, P-ERK1/2 and P-P38 were amplified using the DAB amplification system (#NEL938001EA, Perkin Elmer). For antigen retrieval, paraffin wax-embedded sections were deparaffinized, pressure-cooked for 15 min in antigen unmasking solution (H3300, Vector Laboratories), treated with 3% H_2O_2/PBS for blocking of endogenous peroxidases, washed in PBST (0.05% Tween-20 in PBS) and incubated in TNB Blocking Buffer (NEL702001KT, Perkin Elmer). Sections were then incubated with primary antibodies at 4°C overnight. Nuclei were stained with 4′,6-diamidino-2-phenylindole (DAPI, 6335.1, Carl Roth).

Cellular assays

In vivo cell proliferation rates of E12.5 and E14.5 ureters were assayed by detection of incorporated 5-bromo-2′-deoxyuridine (BrdU) on 5 µm sections (Bussen et al., 2004). Five to 25 sections of each specimen were analyzed. The BrdU labeling index was defined as the number of BrdU-positive nuclei relative to the total number of nuclei detected by DAPI counterstaining in histologically defined compartments of the ureter. Apoptosis in tissues was assessed by the terminal deoxynucleotidyl transferase dUTP nick end labeling (TUNEL) assay using ApopTag Plus Fluorescein In Situ Apoptosis Detection Kit (S7111; Merck) on 5 µm paraffin wax-embedded sections.

In situ hybridization analysis

Section *in situ* hybridization on 10 µm paraffin wax-embedded sections using digoxigenin-labeled antisense riboprobes was performed as previously described (Moorman et al., 2001).

Reverse transcription-polymerase chain reaction (RT-PCR)

RNA extraction and RT-PCR analysis for gene expression was performed on pools of 20 ureters each of E14.5 control and *Pax2-cre/+;Fgfr1*$^{fl/+}$*;Fgfr2*$^{fl/fl}$ embryos. We isolated total RNA using TRIzol (#15596-018, Thermo Fisher Scientific) and synthesized cDNA from total RNA applying RevertAid H Minus reverse transcriptase (#EP0452, Thermo Fisher Scientific) as described previously (Thiesler et al., 2021). The NCBI tool Primer3 version4.1 was used to design specific primers (Table S11) (Untergasser et al., 2012; Werneburg et al., 2015). RT-quantitative (q)PCR of mouse genes was performed in 10 µl 1:2 diluted BIO SyGreen Lo-ROX mix (PCR Biosystems) with 400 nM primers and 1 ng/µl cDNA applying a QuantStudio3 PCR system fluorometric thermal cycler (Thermo Fisher Scientific). Data were processed by QuantStudio data analysis software (version 1.5.1, Thermo Fisher Scientific) using the comparative threshold cycle ($\Delta\Delta C_T$) method.

Microarray analysis

Two independent pools each of control and mutant ureters were used for microarray analysis. Pool sizes were as follows: 50 ureters each from male and female E13.5 *cre*-negative and *Pax2-cre/+;Fgfr1*$^{fl/(+\ or\ fl)}$*;Fgfr2*$^{fl/fl}$ embryos. Total RNA from each pool was extracted using peqGOLD RNApure (30-1010, VWR international) and subsequently processed by the Research Core Unit Transcriptomics of Hannover Medical School. Agilent whole Mouse Genome Oligo v2 (4×44K) Microarrays (G4846A; Agilent Technologies) were used for transcriptome analysis. Normalized expression data were filtered using Microsoft Excel. Functional enrichment analysis for up- and downregulated genes was performed with DAVID 6.8 web-software (david.ncifcrf.gov), and terms were selected based on *P*-value. Microarray data have been deposited in GEO under accession number GSE178093.

Statistics

Statistical analysis was performed using the unpaired, two-tailed Student's *t*-test (GraphPad Prism version 7.03 and Microsoft Excel). Values are indicated as mean±s.d. $P<0.05$ was considered significant.

Image documentation

Sections were photographed using a DM5000 microscope (Leica Camera) with a Leica DFC300FX digital camera or a Leica DMI6000B microscope with a Leica DFC350FX digital camera. All images were then processed using Adobe Photoshop CS4.

Acknowledgements

We thank Rolf Kemler for the anti-CDH1 antiserum. Microarray data used in this publication were generated by the Research Core Unit Genomics (RCUG) at Hannover Medical School. Nurullah Aydoğdu was supported by the Hannover Biomedical Research School (HBRS) and the MD/PhD program Molecular Medicine.

Competing interests

The authors declare no competing or financial interests.

Author contributions

Conceptualization: M.M., L.D., A.K.; Methodology: M.M., L.D., H.T., M.-O.T.; Software: M.-O.T.; Validation: L.D.; Formal analysis: M.M., L.D., N.A., H.T., P.Z.,

M.-O.T.; Investigation: M.M., L.D., C.R., N.A., H.T., P.Z.; Data curation: M.-O.T.; Writing - original draft: M.M., L.D., H.T., A.K.; Writing - review & editing: M.M., L.D., C.R., N.A., H.T., P.Z., H.H., A.K.; Visualization: L.D.; Supervision: C.R., H.H., A.K.; Project administration: A.K.; Funding acquisition: A.K.

Funding
This work was supported by a grant from by the Deutsche Forschungsgemeinschaft (German Research Foundation) (DFG KI 728/12-1 to A.K.).

Data availability
Microarray data have been deposited in GEO under accession number GSE178093.

Peer review history
The peer review history is available online at https://journals.biologists.com/dev/article-lookup/doi/10.1242/dev.200021.

References

Bagai, S., Rubio, E., Cheng, J. F., Sweet, R., Thomas, R., Fuchs, E., Grady, R., Mitchell, M. and Bassuk, J. A. (2002). Fibroblast growth factor-10 is a mitogen for urothelial cells. *J. Biol. Chem.* **277**, 23828-23837. doi:10.1074/jbc.M201658200

Balsara, Z. R. and Li, X. (2017). Sleeping beauty: awakening urothelium from its slumber. *Am. J. Physiol. Renal Physiol.* **312**, F732-F743. doi:10.1152/ajprenal.00337.2016

Bel-Vialar, S., Itasaki, N. and Krumlauf, R. (2002). Initiating Hox gene expression: in the early chick neural tube differential sensitivity to FGF and RA signaling subdivides the HoxB genes in two distinct groups. *Development* **129**, 5103-5115. doi:10.1242/dev.129.22.5103

Bohnenpoll, T. and Kispert, A. (2014). Ureter growth and differentiation. *Semin. Cell Dev. Biol.* **36**, 21-30. doi:10.1016/j.semcdb.2014.07.014

Bohnenpoll, T., Feraric, S., Nattkemper, M., Weiss, A.-C., Rudat, C., Meuser, M., Trowe, M.-O. and Kispert, A. (2017a). Diversification of cell lineages in ureter development. *J. Am. Soc. Nephrol.* **28**, 1792-1801. doi:10.1681/ASN.2016080849

Bohnenpoll, T., Weiss, A.-C., Labuhn, M., Lüdtke, T. H., Trowe, M.-O. and Kispert, A. (2017b). Retinoic acid signaling maintains epithelial and mesenchymal progenitors in the developing mouse ureter. *Sci. Rep.* **7**, 14803. doi:10.1038/s41598-017-14790-2

Bohnenpoll, T., Wittern, A. B., Mamo, T. M., Weiss, A.-C., Rudat, C., Kleppa, M.-J., Schuster-Gossler, K., Wojahn, I., Lüdtke, T. H.-W., Trowe, M.-O. et al. (2017c). A SHH-FOXF1-BMP4 signaling axis regulating growth and differentiation of epithelial and mesenchymal tissues in ureter development. *PLoS Genet.* **13**, e1006951. doi:10.1371/journal.pgen.1006951

Bussen, M., Petry, M., Schuster-Gossler, K., Leitges, M., Gossler, A. and Kispert, A. (2004). The T-box transcription factor Tbx18 maintains the separation of anterior and posterior somite compartments. *Genes Dev.* **18**, 1209-1221. doi:10.1101/gad.300104

Cancilla, B., Ford-Perriss, M. D. and Bertram, J. F. (1999). Expression and localization of fibroblast growth factors and fibroblast growth factor receptors in the developing rat kidney. *Kidney Int.* **56**, 2025-2039. doi:10.1046/j.1523-1755.1999.00781.x

Chen, J. K., Taipale, J., Cooper, M. K. and Beachy, P. A. (2002). Inhibition of Hedgehog signaling by direct binding of cyclopamine to Smoothened. *Genes Dev.* **16**, 2743-2748. doi:10.1101/gad.1025302

Cheng, W., Jacobs, W. B., Zhang, J. J., Moro, A., Park, J.-H., Kushida, M., Qiu, W., Mills, A. A. and Kim, P. C. W. (2006). DeltaNp63 plays an anti-apoptotic role in ventral bladder development. *Development* **133**, 4783-4792. doi:10.1242/dev.02621

Cooper, M. K., Porter, J. A., Young, K. E. and Beachy, P. A. (1998). Teratogen-mediated inhibition of target tissue response to Shh signaling. *Science* **280**, 1603-1607. doi:10.1126/science.280.5369.1603

Cunha, G. R., Young, P., Higgins, S. J. and Cooke, P. S. (1991). Neonatal seminal vesicle mesenchyme induces a new morphological and functional phenotype in the epithelia of adult ureter and ductus deferens. *Development* **111**, 145-158. doi:10.1242/dev.111.1.145

Dalghi, M. G., Montalbetti, N., Carattino, M. D. and Apodaca, G. (2020). The Urothelium: Life in a Liquid Environment. *Physiol. Rev.* **100**, 1621-1705. doi:10.1152/physrev.00041.2019

Dudley, A. T., Godin, R. E. and Robertson, E. J. (1999). Interaction between FGF and BMP signaling pathways regulates development of metanephric mesenchyme. *Genes Dev.* **13**, 1601-1613. doi:10.1101/gad.13.12.1601

Gandhi, D., Molotkov, A., Batourina, E., Schneider, K., Dan, H., Reiley, M., Laufer, E., Metzger, D., Liang, F., Liao, Y. et al. (2013). Retinoid signaling in progenitors controls specification and regeneration of the urothelium. *Dev. Cell* **26**, 469-482. doi:10.1016/j.devcel.2013.07.017

Girshovich, A., Vinsonneau, C., Perez, J., Vandermeersch, S., Verpont, M.-C., Placier, S., Jouanneau, C., Letavernier, E., Baud, L. and Haymann, J.-P. (2012). Ureteral obstruction promotes proliferation and differentiation of the renal urothelium into a bladder-like phenotype. *Kidney Int.* **82**, 428-435. doi:10.1038/ki.2012.110

Guo, J., Zhang, T. and Dou, D. (2019). Knockdown of HOXB8 inhibits tumor growth and metastasis by the inactivation of Wnt/beta-catenin signaling pathway in osteosarcoma. *Eur. J. Pharmacol.* **854**, 22-27. doi:10.1016/j.ejphar.2019.04.004

Hanafusa, H., Torii, S., Yasunaga, T. and Nishida, E. (2002). Sprouty1 and Sprouty2 provide a control mechanism for the Ras/MAPK signalling pathway. *Nat. Cell Biol.* **4**, 850-858. doi:10.1038/ncb867

Hoch, R. V. and Soriano, P. (2006). Context-specific requirements for Fgfr1 signaling through Frs2 and Frs3 during mouse development. *Development* **133**, 663-673. doi:10.1242/dev.02242

Hollnagel, A., Oehlmann, V., Heymer, J., Rüther, U. and Nordheim, A. (1999). Id genes are direct targets of bone morphogenetic protein induction in embryonic stem cells. *J. Biol. Chem.* **274**, 19838-19845. doi:10.1074/jbc.274.28.19838

Huang, J., Dattilo, L. K., Rajagopal, R., Liu, Y., Kaartinen, V., Mishina, Y., Deng, C.-X., Umans, L., Zwijsen, A., Roberts, A. B. et al. (2009). FGF-regulated BMP signaling is required for eyelid closure and to specify conjunctival epithelial cell fate. *Development* **136**, 1741-1750. doi:10.1242/dev.034082

Igarashi, M., Finch, P. W. and Aaronson, S. A. (1998). Characterization of recombinant human fibroblast growth factor (FGF)-10 reveals functional similarities with keratinocyte growth factor (FGF-7). *J. Biol. Chem.* **273**, 13230-13235. doi:10.1074/jbc.273.21.13230

Jans, D. A. (1994). Nuclear signaling pathways for polypeptide ligands and their membrane receptors? *FASEB J.* **8**, 841-847. doi:10.1096/fasebj.8.11.8070633

Kelly, R. G., Brown, N. A. and Buckingham, M. E. (2001). The arterial pole of the mouse heart forms from Fgf10-expressing cells in pharyngeal mesoderm. *Dev. Cell.* **1**, 435-440. doi:10.1016/S1534-5807(01)00040-5

Kuschert, S., Rowitch, D. H., Haenig, B., McMahon, A. P. and Kispert, A. (2001). Characterization of Pax-2 regulatory sequences that direct transgene expression in the Wolffian duct and its derivatives. *Dev. Biol.* **229**, 128-140. doi:10.1006/dbio.2000.9971

Li, X. J., Hu, B. Y., Jones, S. A., Zhang, Y. S., Lavaute, T., Du, Z. W. and Zhang, S. C. (2008). Directed differentiation of ventral spinal progenitors and motor neurons from human embryonic stem cells by small molecules. *Stem Cells* **26**, 886-893. doi:10.1634/stemcells.2007-0620

Liu, K. J. and Harland, R. M. (2003). Cloning and characterization of Xenopus Id4 reveals differing roles for Id genes. *Dev. Biol.* **264**, 339-351. doi:10.1016/j.ydbio.2003.08.017

Mamo, T. M., Wittern, A. B., Kleppa, M.-J., Bohnenpoll, T., Weiss, A.-C. and Kispert, A. (2017). BMP4 uses several different effector pathways to regulate proliferation and differentiation in the epithelial and mesenchymal tissue compartments of the developing mouse ureter. *Hum. Mol. Genet.* **26**, 3553-3563. doi:10.1093/hmg/ddx242

Mendelsohn, C., Ruberte, E., LeMeur, M., Morriss-Kay, G. and Chambon, P. (1991). Developmental analysis of the retinoic acid-inducible RAR-beta 2 promoter in transgenic animals. *Development* **113**, 723-734. doi:10.1242/dev.113.3.723

Mills, C. G., Lawrence, M. L., Munro, D. A. D., Elhendawi, M., Mullins, J. J. and Davies, J. A. (2017). Asymmetric BMP4 signalling improves the realism of kidney organoids. *Sci. Rep.* **7**, 14824. doi:10.1038/s41598-017-14809-8

Mjaatvedt, C. H., Nakaoka, T., Moreno-Rodriguez, R., Norris, R. A., Kern, M. J., Eisenberg, C. A., Turner, D. and Markwald, R. R. (2001). The outflow tract of the heart is recruited from a novel heart-forming field. *Dev. Biol.* **238**, 97-109. doi:10.1006/dbio.2001.0409

Moorman, A. F., Houweling, A. C., de Boer, P. A. J. and Christoffels, V. M. (2001). Sensitive nonradioactive detection of mRNA in tissue sections: novel application of the whole-mount in situ hybridization protocol. *J. Histochem. Cytochem.* **49**, 1-8. doi:10.1177/002215540104900101

Narla, S. T., Bushnell, D. S., Schaefer, C. M., Nouraie, M., Tometich, J. T., Hand, T. W. and Bates, C. M. (2020). Loss of fibroblast growth factor receptor 2 (FGFR2) leads to defective bladder urothelial regeneration after Cyclophosphamide injury. *Am J. Pathol.* **191**, 631-651. doi:10.1016/j.ajpath.2020.12.011

Ornitz, D. M. and Itoh, N. (2015). The fibroblast growth factor signaling pathway. *Wiley Interdiscip. Rev. Dev. Biol.* **4**, 215-266. doi:10.1002/wdev.176

Park, E. J., Watanabe, Y., Smyth, G., Miyagawa-Tomita, S., Meyers, E., Klingensmith, J., Camenisch, T., Buckingham, M. and Moon, A. M. (2008). An FGF autocrine loop initiated in second heart field mesoderm regulates morphogenesis at the arterial pole of the heart. *Development* **135**, 3559-3610. doi:10.1242/dev.025437

Peters, K. G., Werner, S., Chen, G. and Williams, L. T. (1992). Two FGF receptor genes are differentially expressed in epithelial and mesenchymal tissues during limb formation and organogenesis in the mouse. *Development* **114**, 233-243. doi:10.1242/dev.114.1.233

Petiot, A., Perriton, C. L., Dickson, C. and Cohn, M. J. (2005). Development of the mammalian urethra is controlled by Fgfr2-IIIb. *Development* **132**, 2441-2450. doi:10.1242/dev.01778

Pignon, J. C., Grisanzio, C., Geng, Y., Song, J., Shivdasani, R. A. and Signoretti, S. (2013). p63-expressing cells are the stem cells of developing prostate, bladder, and colorectal epithelia. *Proc. Natl. Acad. Sci. USA* **110**, 8105-8110. doi:10.1073/pnas.1221216110

Revest, J.-M., Spencer-Dene, B., Kerr, K., De Moerlooze, L., Rosewell, I. and Dickson, C. (2001). Fibroblast growth factor receptor 2-IIIb acts upstream of Shh and Fgf4 and is required for limb bud maintenance but not for the induction of Fgf8, Fgf10, Msx1, or Bmp4. *Dev. Biol.* **231**, 47-62. doi:10.1006/dbio.2000.0144

Rice, R., Spencer-Dene, B., Connor, E. C., Gritli-Linde, A., McMahon, A. P., Dickson, C., Thesleff, I. and Rice, D. P. C. (2004). Disruption of Fgf10/Fgfr2b-coordinated epithelial-mesenchymal interactions causes cleft palate. *J. Clin. Invest.* **113**, 1692-1700. doi:10.1172/JCI20384

Sato, N., Meijer, L., Skaltsounis, L., Greengard, P. and Brivanlou, A. H. (2004). Maintenance of pluripotency in human and mouse embryonic stem cells through activation of Wnt signaling by a pharmacological GSK-3-specific inhibitor. *Nat. Med.* **10**, 55-63. doi:10.1038/nm979

Schindelin, J., Arganda-Carreras, I., Frise, E., Kaynig, V., Longair, M., Pietzsch, T., Preibisch, S., Rueden, C., Saalfeld, S., Schmid, B. et al. (2012). Fiji: an open-source platform for biological-image analysis. *Nat. Methods* **9**, 676-682. doi:10.1038/nmeth.2019

Sims-Lucas, S., Cusack, B., Eswarakumar, V. P., Zhang, J., Wang, F. and Bates, C. M. (2011). Independent roles of Fgfr2 and Frs2alpha in ureteric epithelium. *Development* **138**, 1275-1280. doi:10.1242/dev.062158

Tash, J. A., David, S. G., Vaughan, E. E. and Herzlinger, D. A. (2001). Fibroblast growth factor-7 regulates stratification of the bladder urothelium. *J. Urol.* **166**, 2536-2541. doi:10.1016/S0022-5347(05)65630-3

Terakawa, J., Rocchi, A., Serna, V. A., Bottinger, E. P., Graff, J. M. and Kurita, T. (2016). FGFR2IIIb-MAPK activity is required for epithelial cell fate decision in the lower mullerian duct. *Mol. Endocrinol.* **30**, 783-795. doi:10.1210/me.2016-1027

Thiesler, H., Beimdiek, J. and Hildebrandt, H. (2021). Polysialic acid and Siglec-E orchestrate negative feedback regulation of microglia activation. *Cell. Mol. Life Sci.* **78**, 1637-1653. doi:10.1007/s00018-020-03601-z

Trowe, M.-O., Airik, R., Weiss, A.-C., Farin, H. F., Foik, A. B., Bettenhausen, E., Schuster-Gossler, K., Taketo, M. M. and Kispert, A. (2012). Canonical Wnt signaling regulates smooth muscle precursor development in the mouse ureter. *Development* **139**, 3099-3108. doi:10.1242/dev.077388

Trowe, M.-O., Maier, H., Petry, M., Schweizer, M., Schuster-Gossler, K. and Kispert, A. (2011). Impaired stria vascularis integrity upon loss of E-cadherin in basal cells. *Dev. Biol.* **359**, 95-107. doi:10.1016/j.ydbio.2011.08.030

Untergasser, A., Cutcutache, I., Koressaar, T., Ye, J., Faircloth, B. C., Remm, M. and Rozen, S. G. (2012). Primer3-new capabilities and interfaces. *Nucleic Acids Res.* **40**, e115. doi:10.1093/nar/gks596

Walker, K. A., Sims-Lucas, S. and Bates, C. M. (2016). Fibroblast growth factor receptor signaling in kidney and lower urinary tract development. *Pediatr. Nephrol.* **31**, 885-895. doi:10.1007/s00467-015-3151-1

Wang, G. J., Brenner-Anantharam, A., Vaughan, E. D. and Herzlinger, D. (2009). Antagonism of BMP4 signaling disrupts smooth muscle investment of the ureter and ureteropelvic junction. *J. Urol.* **181**, 401-407. doi:10.1016/j.juro.2008.08.117

Wang, C., Ross, W. T. and Mysorekar, I. U. (2017). Urothelial generation and regeneration in development, injury, and cancer. *Dev. Dyn.* **246**, 336-343. doi:10.1002/dvdy.24487

Wang, T., Lin, F., Sun, X., Jiang, L., Mao, R., Zhou, S., Shang, W., Bi, R., Lu, F. and Li, S. (2019). HOXB8 enhances the proliferation and metastasis of colorectal cancer cells by promoting EMT via STAT3 activation. *Cancer Cell Int.* **19**, 3. doi:10.1186/s12935-018-0717-6

Weiss, R. M., Guo, S., Shan, A., Shi, H., Romano, R.-A., Sinha, S., Cantley, L. G. and Guo, J.-K. (2013). Brg1 determines urothelial cell fate during ureter development. *J. Am. Soc. Nephrol.* **24**, 618-626. doi:10.1681/ASN.2012090902

Weiss, A. C., Bohnenpoll, T., Kurz, J., Blank, P., Airik, R., Ludtke, T. H., Kleppa, M. J., Deuper, L., Kaiser, M., Mamo, T. M. et al. (2019). Delayed onset of smooth muscle cell differentiation leads to hydroureter formation in mice with conditional loss of the zinc finger transcription factor gene Gata2 in the ureteric mesenchyme. *J. Pathol.* **248**, 452-463. doi:10.1002/path.5270

Werneburg, S., Buettner, F. F., Mühlenhoff, M. and Hildebrandt, H. (2015). Polysialic acid modification of the synaptic cell adhesion molecule SynCAM 1 in human embryonic stem cell-derived oligodendrocyte precursor cells. *Stem Cell Res.* **14**, 339-346. doi:10.1016/j.scr.2015.03.001

Yamany, T., Van Batavia, J. and Mendelsohn, C. (2014). Formation and regeneration of the urothelium. *Curr. Opin. Organ Transplant.* **19**, 323-330. doi:10.1097/MOT.0000000000000084

Yang, X., Liaw, L., Prudovsky, I., Brooks, P. C., Vary, C., Oxburgh, L. and Friesel, R. (2015). Fibroblast growth factor signaling in the vasculature. *Curr. Atheroscler. Rep.* **17**, 509. doi:10.1007/s11883-015-0509-6

Yu, J., Carroll, T. J. and McMahon, A. P. (2002). Sonic hedgehog regulates proliferation and differentiation of mesenchymal cells in the mouse metanephric kidney. *Development* **129**, 5301-5312. doi:10.1242/dev.129.22.5301

Yu, K., Xu, J., Liu, Z., Sosic, D., Shao, J., Olson, E. N., Towler, D. A. and Ornitz, D. M. (2003). Conditional inactivation of FGF receptor 2 reveals an essential role for FGF signaling in the regulation of osteoblast function and bone growth. *Development* **130**, 3063-3074. doi:10.1242/dev.00491

Zhang, D., Kosman, J., Carmean, N., Grady, R. and Bassuk, J. A. (2006). FGF-10 and its receptor exhibit bidirectional paracrine targeting to urothelial and smooth muscle cells in the lower urinary tract. *Am. J. Physiol. Renal Physiol.* **291**, F481-F494. doi:10.1152/ajprenal.00025.2006

Zhao, H., Kegg, H., Grady, S., Truong, H.-T., Robinson, M. L., Baum, M. and Bates, C. M. (2004). Role of fibroblast growth factor receptors 1 and 2 in the ureteric bud. *Dev. Biol.* **276**, 403-415. doi:10.1016/j.ydbio.2004.09.002

Zimmerman, L. B., De Jesus-Escobar, J. M. and Harland, R. M. (1996). The Spemann organizer signal noggin binds and inactivates bone morphogenetic protein 4. *Cell* **86**, 599-606. doi:10.1016/S0092-8674(00)80133-6

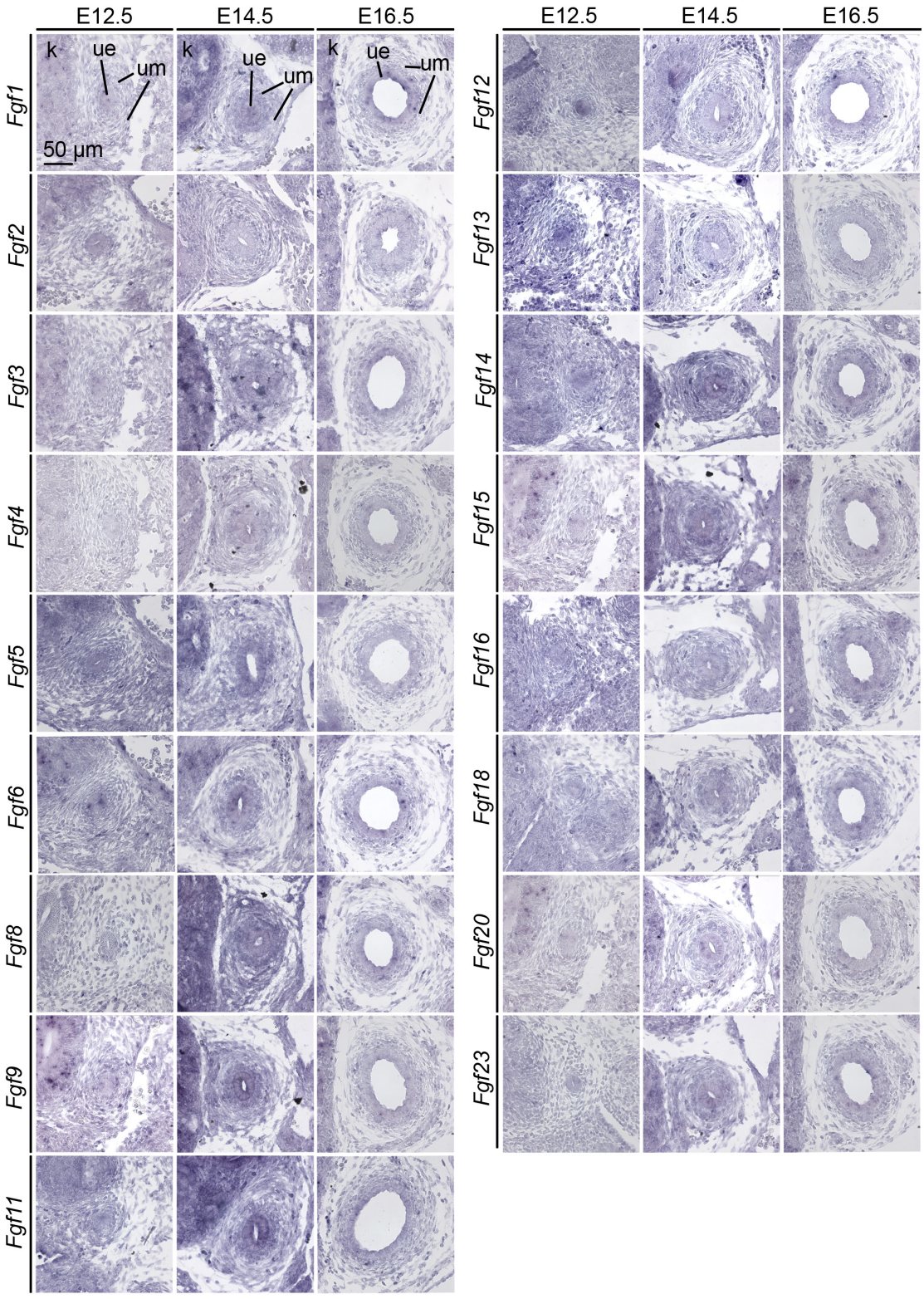

Fig. S1. FGF ligand genes do not show specific expression in the mesenchymal or the epithelial compartment of the early ureter. RNA *in situ* hybridization analysis on transverse sections through the posterior trunk region at the proximal (kidney) level of the ureter for expression of genes encoding FGF ligand genes in wildtype embryos from E12.5 to E16.5. Due to expanded colorimetric detection a homogenous bluish background developed in most cases, but no specific signal was detected in the UE or the UM for any of the probes. n>=3 for all probes and stages. k, kidney; ue, ureteric epithelium; um, ureteric mesenchyme.

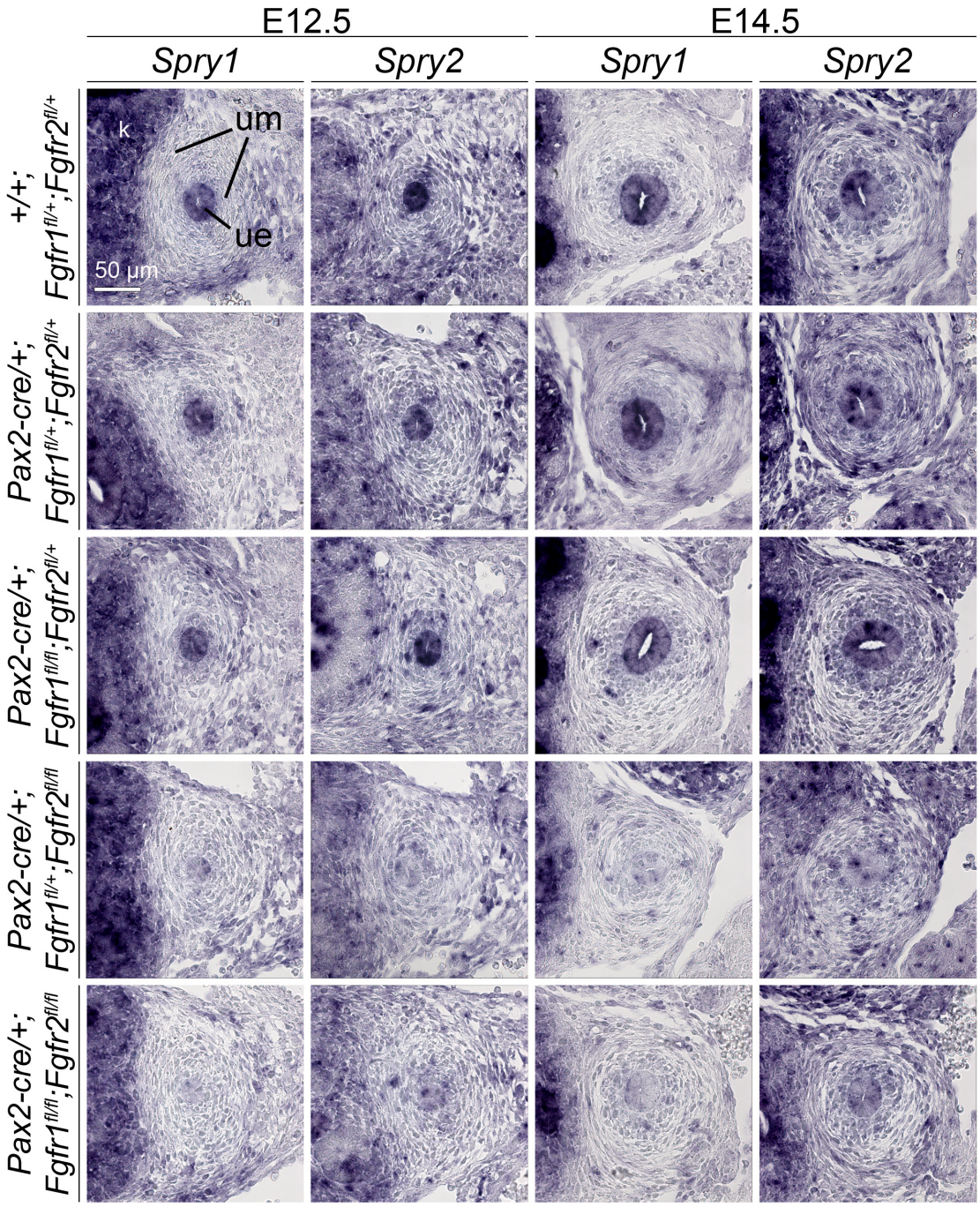

Fig. S2. FGF signaling is specifically diminished in the UE of embryos with conditional loss of *Fgfr2* in this tissue. RNA *in situ* hybridization analysis of expression of transcriptional targets of FGF signaling (*Spry1*, *Spry2*) on transverse sections through the posterior trunk region at the proximal level of the ureter of E12.5 and E14.5 embryos with conditional loss of *Fgfr1* and/or *Fgfr2*. n>=3 for all probes, stages and genotypes. k, kidney; ue, ureteric epithelium; um, ureteric mesenchyme.

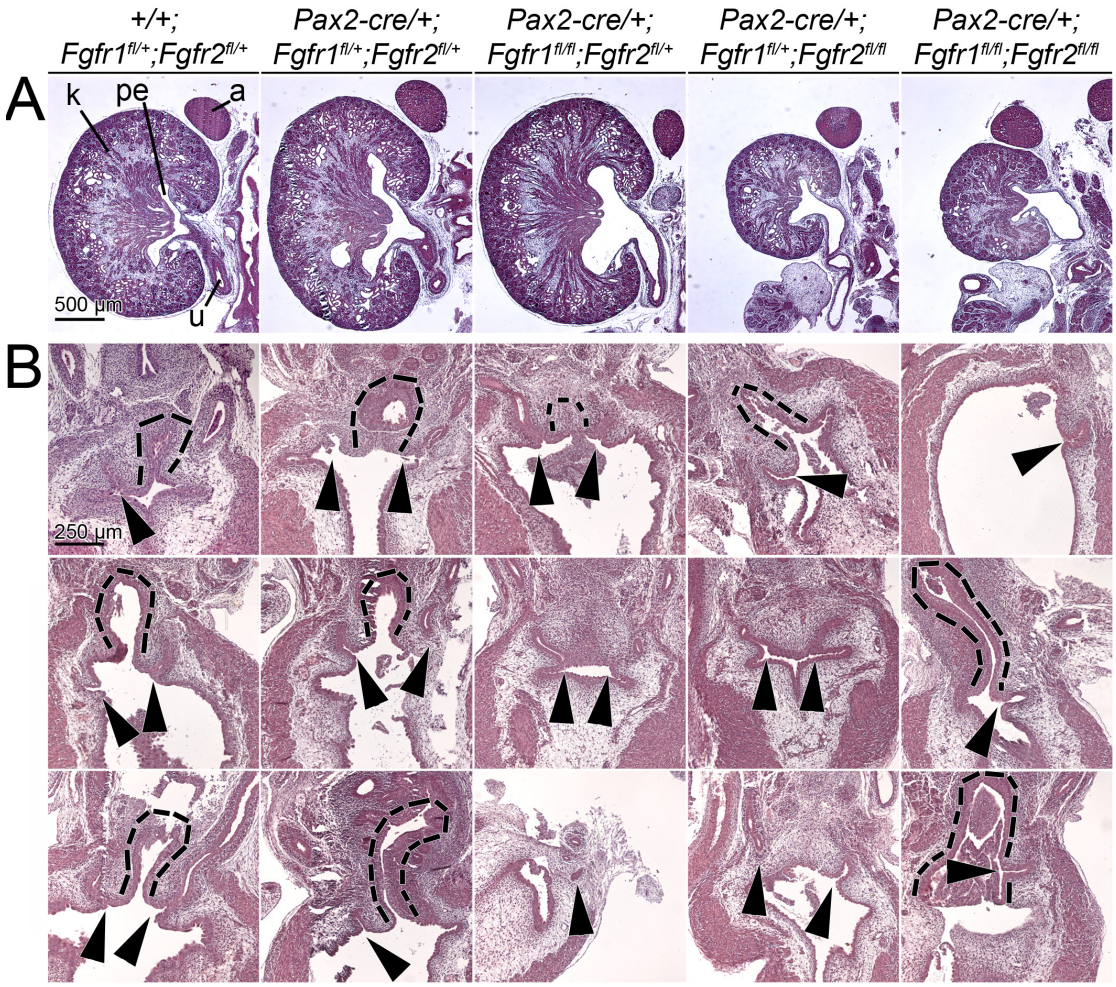

Fig. S3. Histological analysis of the urogenital system of mice with conditional loss of *Fgfr1* and/or *Fgfr2* in the UE. HE staining of sagittal sections of the kidney (A) and the ureter insertion into the bladder (B) at E18.5. (B) Dotted lines mark the urethra; arrowheads mark the ureter insertion. Note the blind ending ureter in the third *Pax2-cre/+;Fgfr1*$^{fl/fl}$*;Fgfr2*$^{fl/+}$ specimen, and the urethral insertion in the third *Pax2-cre/+;Fgfr1*$^{fl/+}$*;Fgfr2*$^{fl/fl}$ specimen. n>=3 for all genotypes. a, adrenal; k, kidney; pe, pelvis; u, ureter.

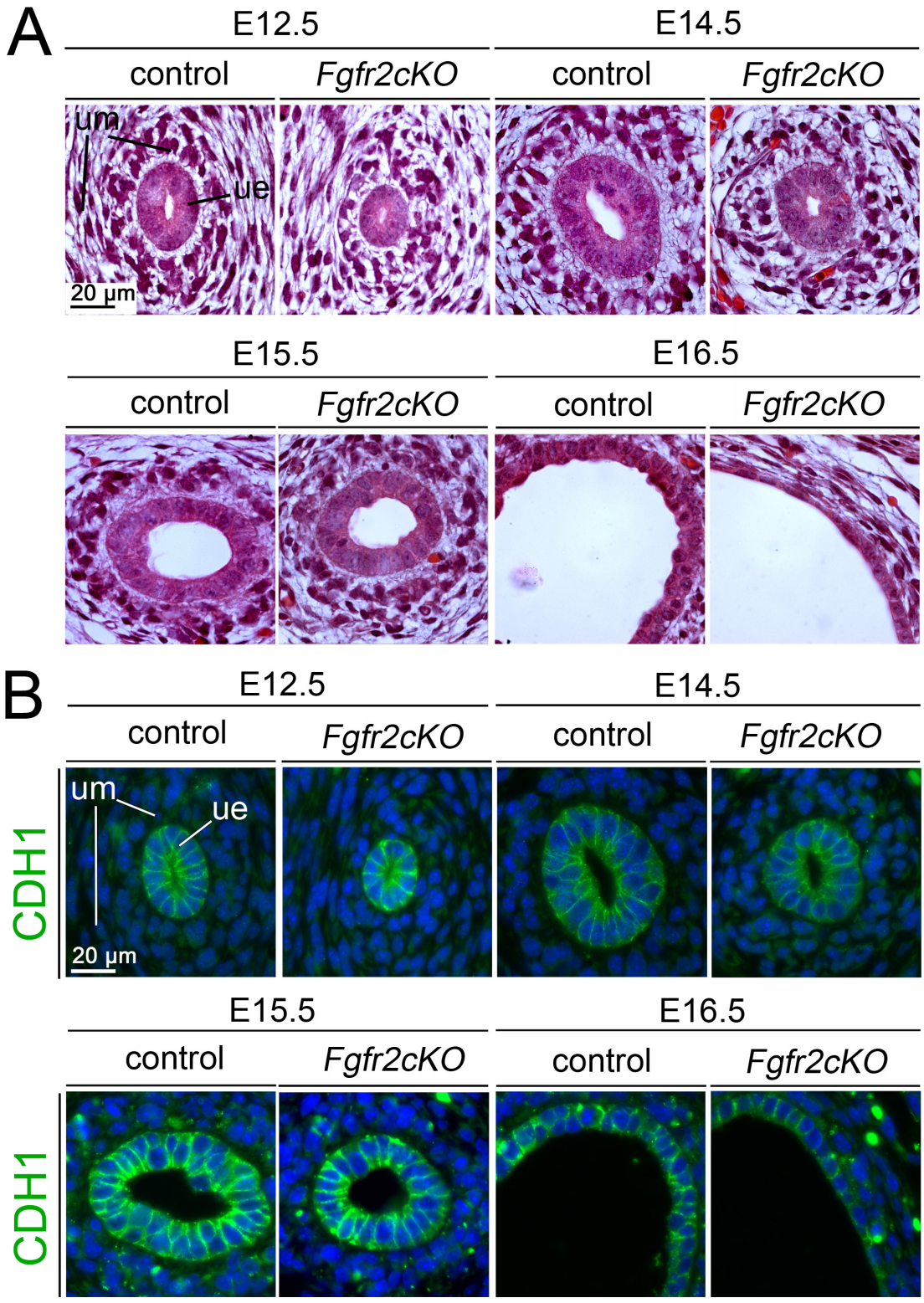

Fig. S4. *Fgfr2cKO* ureters are hypoplastic and exhibit reduced stratification in development. (Higher magnification of images shown in Fig. 3A,B). (A) Hematoxylin and Eosin (HE) staining of transverse sections of the proximal region of the developing ureter at the indicated stages. (B) Analysis of CDH1 expression by immunofluorescence on adjacent sections. Nuclei are counter-stained with DAPI (blue). n>=3, for all probes, assays and genotypes. ue, ureteric epithelium; um, ureteric mesenchyme.

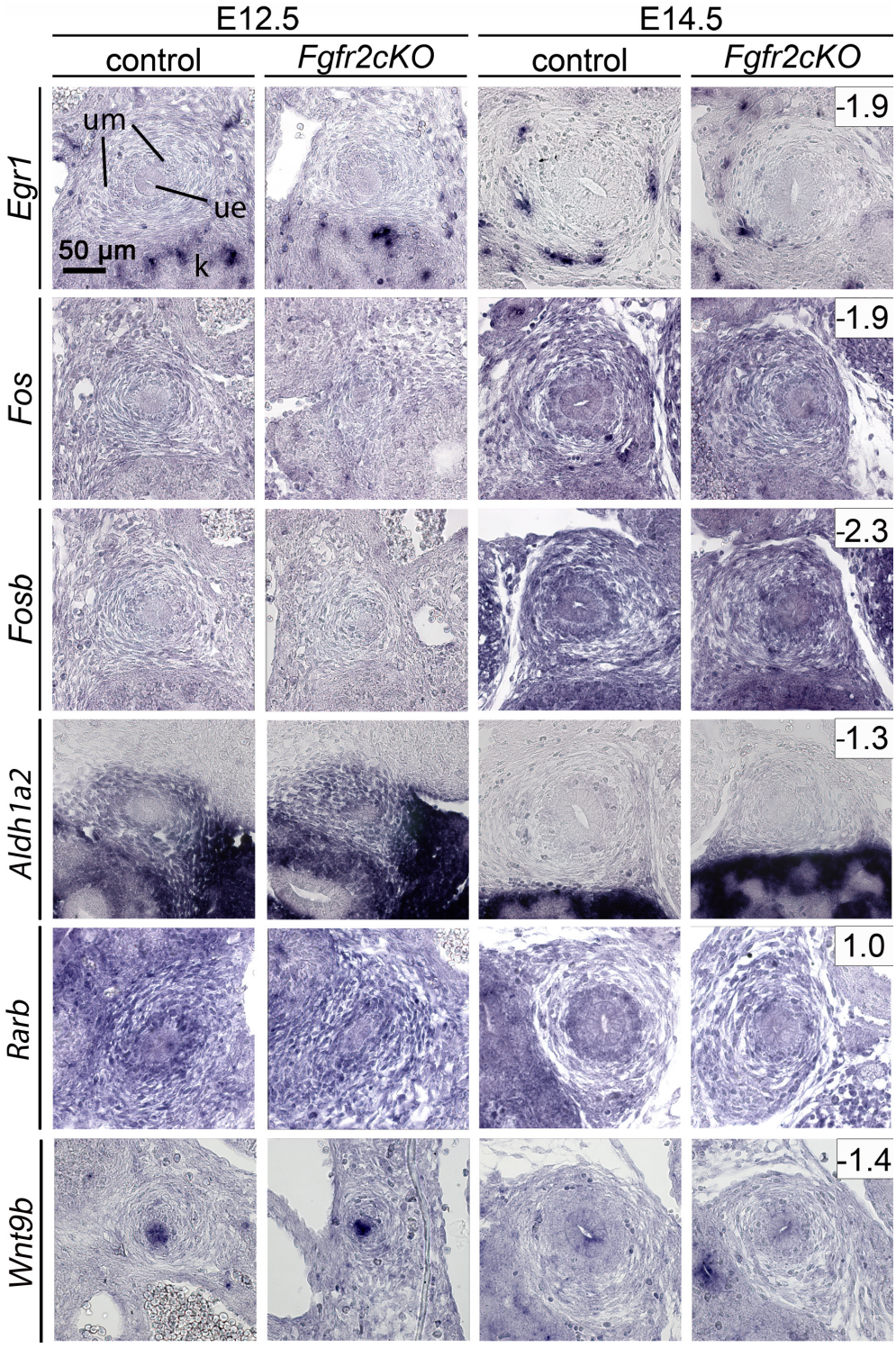

Fig. S5. Expression of immediate early genes, of mesenchymal RA signaling components and of *Wnt9b* is unchanged in *Fgfr2cKO* ureters at E12.5 and E14.5. *In situ* hybridization analysis on transverse sections of the proximal ureter of E12.5 and E14.5 control and *Fgfr2cKO* embryos for expression of immediate early genes (*Egr1, Fos, Fosb)*, of RA signaling components in the UM (*Aldh1a2*, *Rarb*), and of *Wnt9b*. Numbers indicate fold change in the E13.5 microarray analysis. n>=3 for all probes and genotypes k, kidney; ue, ureteric epithelium; um, ureteric mesenchyme.

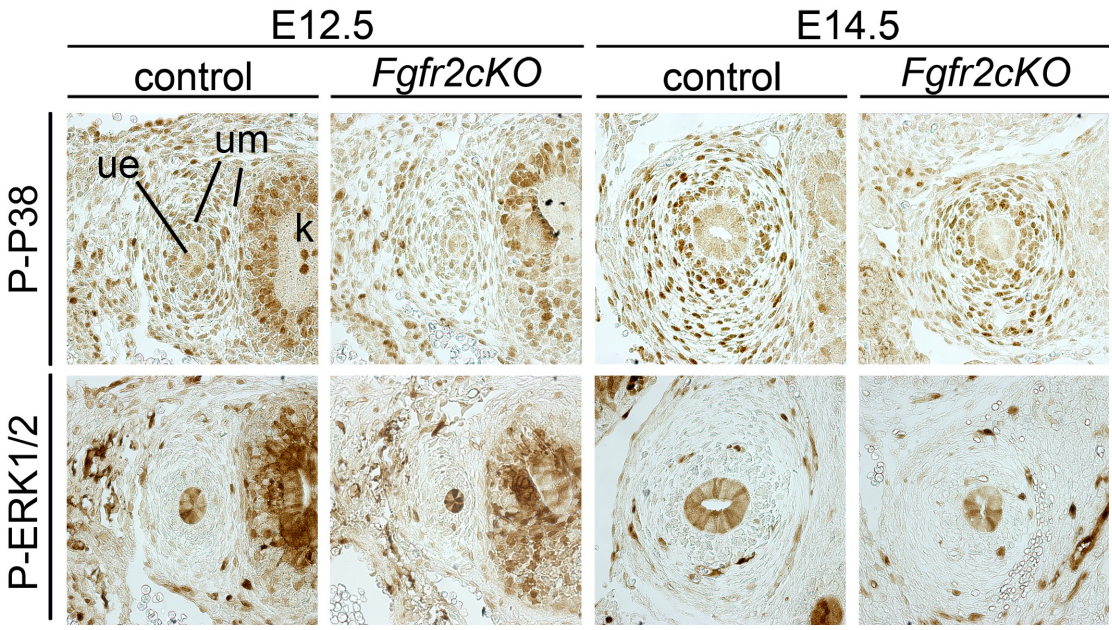

Fig. S6. Phosphorylation of P38 and of ERK1/2 is not changed in *Fgfr2cKO* ureters. Immunohistochemical detection of activated, i.e. phosphorylated forms of cytoplasmic effectors of BMP4 signaling (P-P38, P-ERK1/2) on transverse sections of the proximal ureter of E12.5 and E14.5 control and *Fgfr2cKO* embryos. n>=3 for all probes, genotypes and stages. k, kidney; ue, ureteric epithelium; um, ureteric mesenchyme.

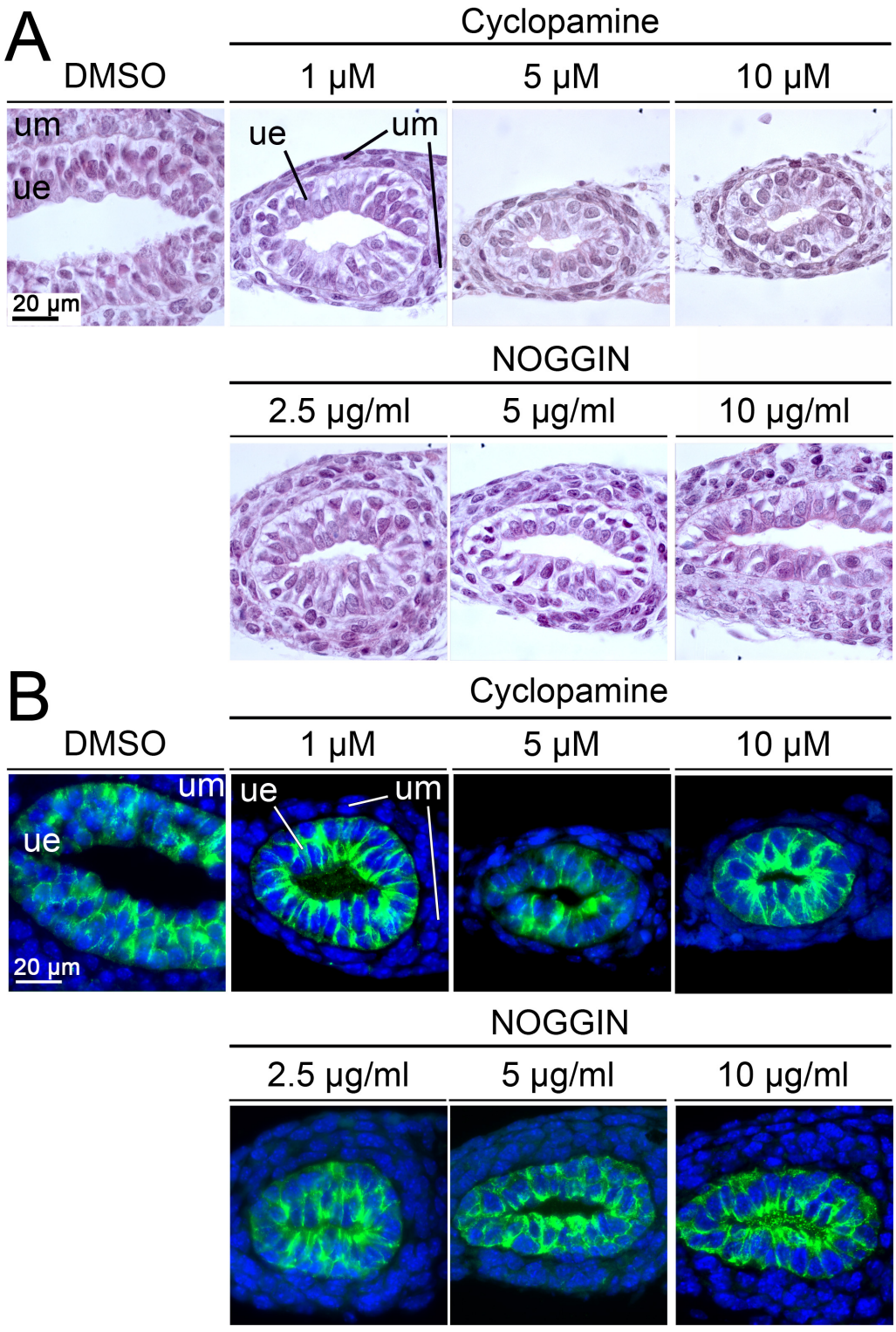

Fig. S7. Inhibition of SHH or BMP4 signaling leads dose-dependently to hypoplastic ureters with reduced stratification. (Higher magnification of images shown in Fig. 6A,B). (A,B) E13.5 wildtype ureters were cultured for 4 days with increasing concentrations of the SHH signaling inhibitor cyclopamine or the BMP4 antagonist NOGGIN, and transverse sections of the proximal region were analyzed by Hematoxylin and Eosin staining (A) and by immunofluorescence for expression of the epithelial marker CDH1. Nuclei are counter-stained with DAPI (blue). n>=3, for all probes, assays and genotypes. ue, ureteric epithelium; um, ureteric mesenchyme.

Table S1. Genotype distribution of embryos obtained from matings of *Pax2-cre/+;Fgfr1fl/;Fgfr2fl/+* males with *Fgfr1fl/fl;Fgfr2fl/fl* females at E12.5, E14.5, E16.5 and E18.5.

Click here to download Table S1

Table S2. A. Distribution of phenotypic changes in urogenital systems of E18.5 embryos obtained from matings of *Pax2-cre/+; Fgfr1fl/;Fgfr2fl/+* males with *Fgfr1fl/fl;Fgfr2fl/fl* females.

Click here to download Table S2

Table S3. Quantification of the BrdU incorporation assay of proximal sections of control and *Fgfr2cKO* ureters at E12.5 and E14.5.

Click here to download Table S3

Table S4. List of genes with increased expression in the microarray of E13.5 ureters of *Fgfr2cKO* and control embryos. Shown are the gene names, the intensity of the two control and mutant ureter samples, the individual and the average fold change (FC).

Click here to download Table S4

Table S5. List of genes with decreased expression in the microarray of E13.5 ureters of *Fgfr2cKO* and control embryos. Shown are the gene names, the intensity of the two control and mutant ureter samples, the individual and the average fold change (FC).

Click here to download Table S5

Table S6. Functional annotation by DAVID for genes with increased expression in the microarray of E13.5 *Fgfr2cKO* ureters.

Click here to download Table S6

Table S7. Functional annotation by DAVID for genes with decreased expression in the microarray of E13.5 *Fgfr2cKO* ureters.

Click here to download Table S7

Table S8. RT-qPCR analysis of gene expression in E13.5 *Fgfr2cKO* ureters (relates to Figure 4H).

Click here to download Table S8

Table S9. Pharmacological rescue experiments in explants of E13.5 *Fgfr2cKO* ureters cultured for 4 days.

Click here to download Table S9

Table S10. Pharmacological inhibition of SHH and BMP4 signaling in explant cultures of E13.5 ureters. E13.5 wildtype ureters were cultured for 4 days with increasing concentrations of the SHH signaling inhibitor cyclopamine or the BMP4 antagonist NOGGIN.

Click here to download Table S10

Table S11. List of primers for RT-qPCR analysis of gene expression in E13.5 *Fgfr2cKO* ureters.

Click here to download Table S11